LAPPEENRANTA UNIVERSITY OF TECHNOLOGY
Faculty of Technology
Department of Electrical Engineering

Master's Thesis

MOBILE SYSTEM FOR PUMP WORKING POINT ESTIMATION

Examiners:
Professor Jero Ahola
M.Sc. Tero Ahonen
Supervisor:
M. Sc. Tero Ahonen

Lappeenranta 26.04.2010

_____

Alexander Golovlev
pr. Staro-Petergofsky 10-3
190020 Saint-Petersburg, Russia
+358465724822

Abstract

Lappeenranta University of Technology

Faculty of Technology

Electrical Engineering

Alexander Golovlev

Mobile system for pump working point estimation

Master's Thesis

2010

71 pages, 67 figures, 9 tables

Examiners: Professor Jero Ahola

M.Sc. Tero Ahonen

Keywords: Pump, induction motor, efficiency, LabVIEW, mobile system

In the current economy situation companies try to reduce their expenses. One of the solutions is to improve the energy efficiency of the processes. It is known that the energy consumption of pumping applications range from 20 up to 50% of the energy usage in the certain industrial plants operations. Some studies have shown that 30% to 50% of energy consumed by pump systems could be saved by changing the pump or the flow control method.

The aim of this thesis is to create a mobile measurement system that can calculate a working point position of a pump drive. This information can be used to determine the efficiency of the pump drive operation and to develop a solution to bring pump's efficiency to a maximum possible value. This can allow a great reduction in the pump drive's life cycle cost.

In the first part of the thesis, a brief introduction in the details of pump drive operation is given. Methods that can be used in the project are presented. Later, the review of available platforms for the project implementation is given. In the second part of the thesis, components of the project are presented. Detailed description for each created component is given. Finally, results of laboratory tests are presented. Acquired results are compared and analyzed. In addition, the operation of created system is analyzed and suggestions for the future development are given.

TABLE OF CONTENTS

SYMBOLS AND ABBREVIATIONS

Greek letters

η	efficiency	(%)
ρ	density of the liquid	(kg/m^3)

Roman letters

F	flux	(Wb)
f	frequency	(Hz)
g	acceleration due to gravity	(m/s^2)
H	head	(m)
i	imaginary unit	
N	number of samples	
n	rotational speed	(rpm)
P	power	(kW)
p	static pressure	(kg/cm^2)
R_m	magnetic reluctance	(1/H)
Q	flow rate	(l/m),(m^3/s)
T	torque	(Nm)
U	voltage	(V)
v	velocity	(m/s)
x_n	input signal	
X_k	output spectrum	

Subscripts

DAQ	data acquisition
DFT	discrete Fourier transform
dyn.	dynamic
FFT	fast Fourier transform
LCC	life cycle cost
MMF	magneto motive force

r	rotor
s	magnetic field
stat	static
VI	virtual instrument
VPF	vane passing frequency
VSD	variable speed drive

1. INTRODUCTION

Pumps are widely used in industry nowadays. Pumping systems account for nearly 20% of the world's electrical energy demand and their share ranges from 25% to 50% of the energy usage in certain industrial plant operations. Pumping systems are widespread; they provide domestic services, commercial and agricultural services, municipal water/wastewater services. They are also widely used in industrial services for food processing, chemical, petrochemical, pharmaceutical and mechanical industries. Although pumps are typically purchased as individual components, they are always a part of a larger process. Energy consumption of the process is strongly affected by the design and dimensioning of the pump used in the process. [1]

The initial purchase price is usually a small part of the overall life cycle costs (LCC) for high usage pumps. LCC typically consist of initial, maintenance, energy and other costs. For pumps larger than 50 kW the most significant are energy and maintenance costs. Their parts of total LCC sum are shown in Figure 1-1. [1]

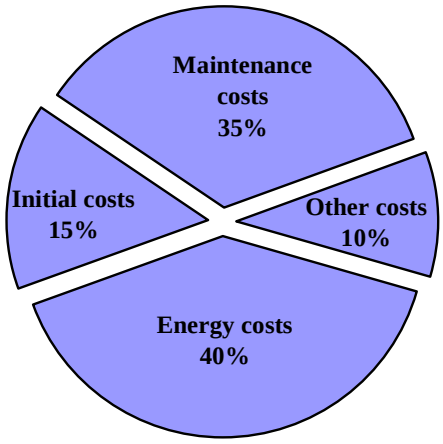

Figure 1-1 Typical life cycle costs for a medium-sized industrial pump. [1]

It is worth mentioning that a typical medium-sized plant spends over $1.4 millions a year to run their pumping systems [2]. In many cases, pumps operate inefficiently, which causes the increase of energy and maintenance costs. Long term

pump operation outside its recommended working region can lead to different fault consequences such as wear out of bearings, impeller, sealing, etc. (Figure 1-2). Pump failure may lead to a shutdown of a production, that would lead to additional notable costs. This kind of operation increases the energy costs of the pump drive usage as pump efficiency is lower than it could be.

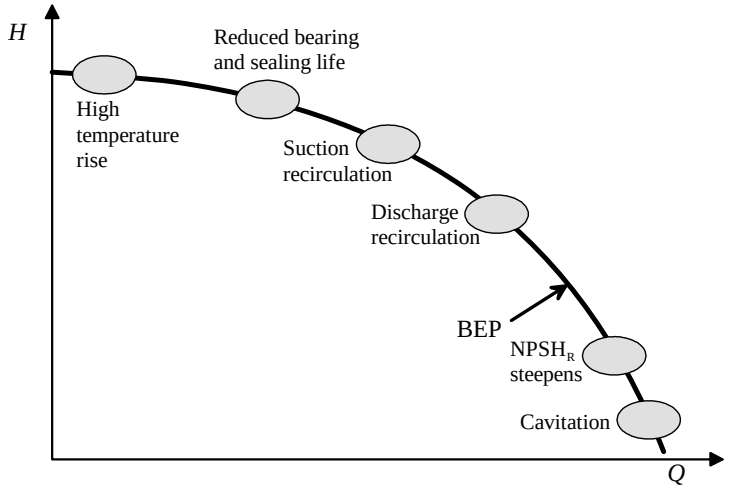

Figure 1-2 Onset of possible adverse effects when operating away from working region [3].

An inefficient and a possibly harmful operation of the pump is the reason why pump operation monitoring is an essential task. If the inefficient operation can be detected at early stage, the resulting increase of energy costs can be avoided by improving the pump characteristics. In addition to the economic reasons, many organizations are becoming increasingly aware of the environmental impact of their businesses, and are considering energy efficiency as one way to reduce emissions and preserve natural resources. [1]

Today there are several systems that provide tools for pump efficiency monitoring, but most of them are fixed systems and they must be permanently installed for a particular pump drive. Figure 1-3 shows an example of commercially available monitoring product.

Figure 1-3 Sulzer pump with IntO™ condition monitoring device. [4]

1.1. Objectives of the work

The purpose of this thesis is to develop a mobile system for pump working point estimation which allows the analysis of pump operation with portable measurement sensors. The system should be capable to save results for future analysis. The logical parts of the system are presented in Figure 1-4. Vibration measurement and flow rate measurement parts are performed by special hardware devices and all other parts are implemented in software.

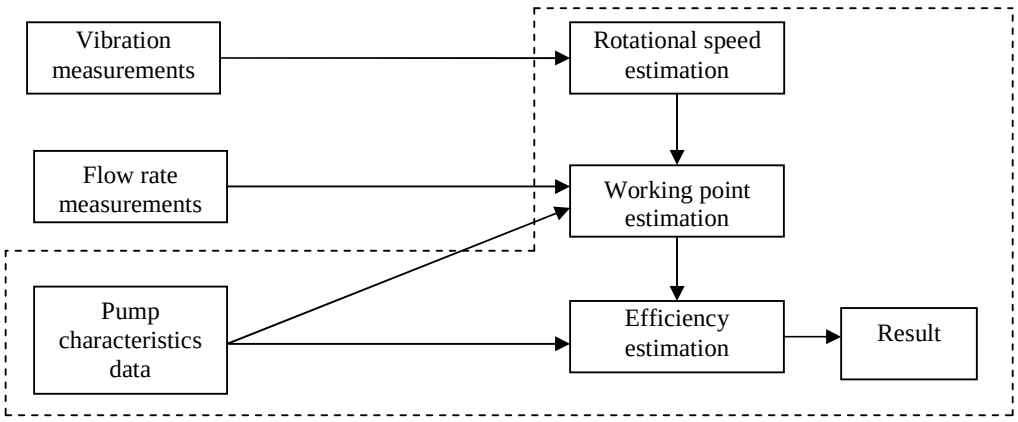

Figure 1-4 Parts of the system. Dashed line shows the software parts.

For the estimation of pump's working point several input parameters are needed: pump's rotational speed, pump's characteristics data and pump's flow.

The rotational speed estimation part of the measurement system has several restrictions. It should be portable, the sensor should be capable of providing results without direct access to the rotating parts of the machine, and the estimation algorithm should provide correct results. According to these restrictions, a suitable sensor is selected. Two speed estimation methods are studied and the correctness of their results is evaluated in series of tests. Tests are conducted on pump drives and fan blowers.

The working point estimation part of the measuring system requires the knowledge about the pump's rotational speed, the pump's flow and pump's characteristic curves. The flow metering methods are not studied in this project. To determine the current pump flow rate, an ultrasonic flow metering device is used. For the convenience a database solution for pump's characteristic curves is utilized. The curves are provided by pump manufacturers.

The efficiency estimation is done upon data provided by working point estimation part and pump's characteristic curves.

The developed system is evaluated for applicability by measurements of two pump drives and a fan drive.

1.2. Outline of the work

Chapter 2 presents a brief intro of pump drives. It describes available types of pumps, principle of operation, basic parameters, characteristic curves and efficiency estimation principles. In the second part of the chapter a similar introduction is given for induction motors.

Chapter 3 is devoted to vibration measurements theory. Firstly a brief explanation is given why the rotational speed is estimated via vibrations. Then, the characteristic vibrations of induction motors and pumps are explained. The methods of frequency estimation are presented.

In **Chapter 4** a platform selection guideline is described. In the beginning of the chapter a brief intro on available hardware platforms is given. Their advantages and disadvantages are presented. Then the brief description of the chosen software

platform is given. After this all the hardware and software parts of the system are described.

Chapter 5 is dedicated to laboratory tests. It starts with the description of test equipment. Then the test results are presented for each drive. Finally, test results are summarized.

Chapter 6 gives a summary of the work. There is an evaluation of thesis results and suggestions for future projects.

2. PARTS OF PUMP DRIVE

This chapter presents a brief intro on pump drives. A typical pump drive consists of a centrifugal pump and an induction motor. In the first part of the chapter, there is the description of available types of pumps, principle of operation, basic parameters, characteristic curves and efficiency estimation principles. The second part gives the description of an induction motor, its principle of operation, parameters and applicable speed control techniques.

2.1. Pumps

Pumps are mechanical devices used for moving liquids from a lower level to a higher one. It is done by creating low pressure at the inlet and high pressure at the outlet of the pump. Because of the low inlet pressure, the liquid rises from the lower level and the high outlet pressure forces it up where it is needed. A pump requires a mover to enable it to impart mechanical energy to the liquid, which ultimately converts into a hydraulic energy.

According to the principle of operation, pumps are divided into two main groups: rotodynamic pumps (centrifugal pumps) and positive displacement pumps. Pumps classification is given in Figure 2-1. [5]

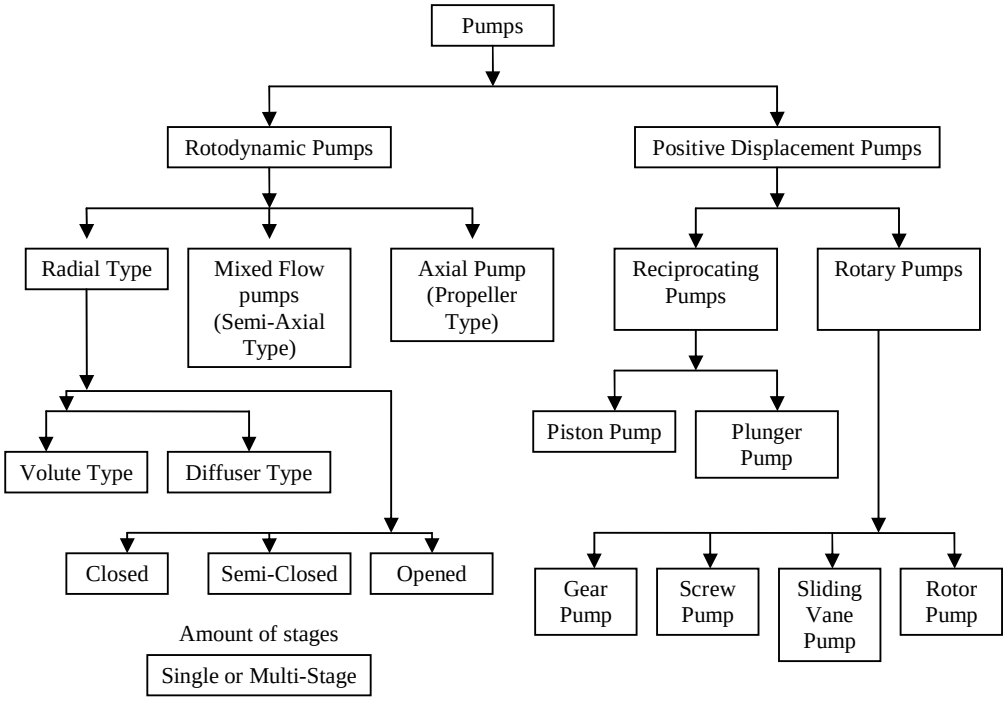

Figure 2-1 Pumps classification [5].

According to [6], rotodynamic (i.e. centrifugal) pumps occupy more than 73% of the market, consequently a radial flow centrifugal pump can be regarded as a typical example of a pump.

2.1.1 Centrifugal pump

A centrifugal pump is one of the simplest pieces of equipment. It employs a centrifugal force to lift liquids from a lower level to a higher one by developing pressure. A simplest type of pump comprises of an impeller fitted on a shaft, rotating in a volute casing. Liquid led into the center of the impeller is picked up by the vanes of the impeller and accelerated to a high velocity by the rotation of the impeller, and discharged by centrifugal force into the casing and then out of the discharge pipe. When liquid is forced away from the center, a vacuum is created and more liquid flows in. [5] All parts of a centrifugal pump are shown in the Figure 2-2.

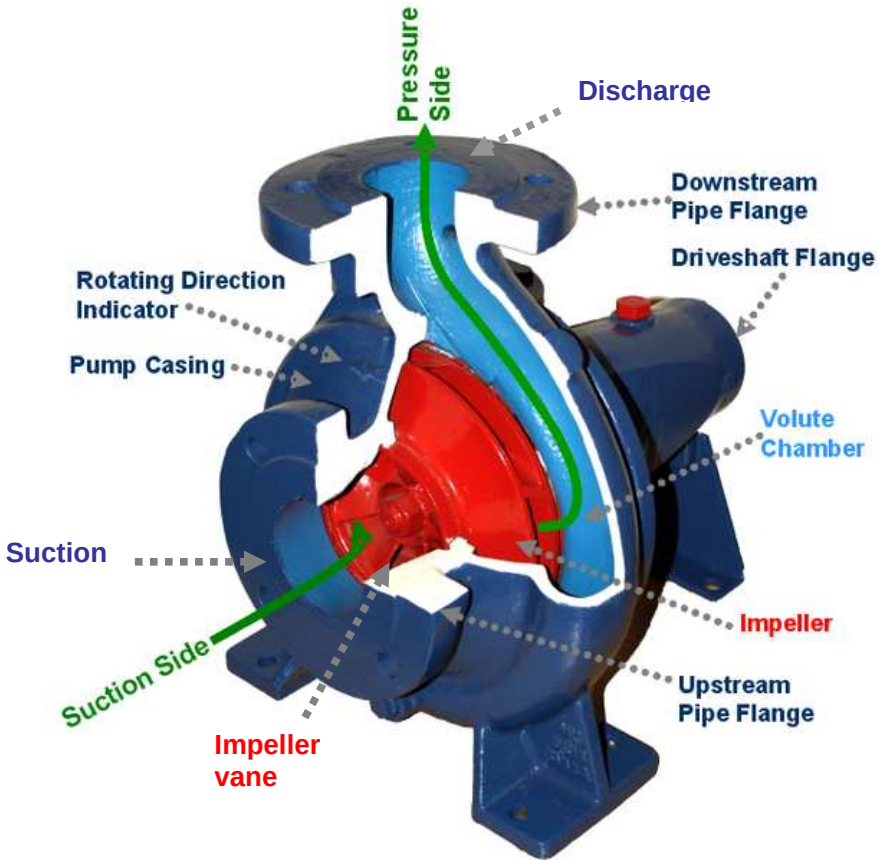

Figure 2-2 Basic parts of a centrifugal pump[7]. Fluid is transported with the impeller from the pump's suction to pump's discharge.

2.1.2 Operational parameters

Operation of a centrifugal pump can be qualified by several variables. In the following typical variables are described.

Flow rate is denoted as ***Q*** and it informs the amount of liquid transferred per unit time. Typically *Q* is the volumetric rate of flow. Different units can be applied to the flow rate, for example it can be measured in liters per minute or cubic meters per second.

Total head is the pressure unit that is commonly used in the hydraulic engineering. Head is denoted as ***H***. It is used to measure the hydraulic energy (i.e.

pressure) created by the pump. Head expresses the amount of pressure as a height of a liquid column. An example of this is shown in Figure 2-3.

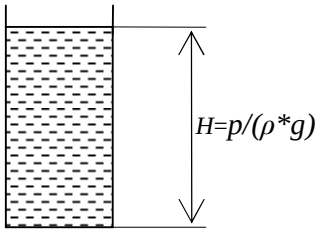

Figure 2-3 Pressure expressed as the height of a liquid column. It is the same regardless of the width or diameter of the tank—the static head is only affected by the height of the liquid.

Pump **efficiency** η is the ratio of hydraulic horsepower P_{out} to the brake horsepower P_{in} required to drive the pump. Hydraulic horsepower equals the hydraulic power available at the discharge of the pump. It can be expressed as

$$P_{out} = \rho \cdot Q \cdot H \cdot g\,, \qquad (2\text{-}1)$$

where ρ is the fluid density and g is the acceleration due to gravity.

Brake horse power is the mechanical power provided by the prime mover. The efficiency of a pump can be calculated if the P_{in} and P_{out} are known.

$$\eta = \frac{\rho \cdot Q \cdot H \cdot g}{P_{in}} \qquad (2\text{-}2)$$

2.1.3 Affinity laws

These laws predict the performance characteristic of a pump when operating at different speeds than the speed at which it has been tested (Figure 2-4). Laws apply to all types of centrifugal and axial flow pumps. [5] In the mathematical relationships given below constant size of impeller is assumed.

$$\frac{Q_1}{Q_2} = \frac{n_1}{n_2} \tag{2-3}$$

$$\frac{H_1}{H_2} = \left(\frac{n_1}{n_2}\right)^2 \tag{2-4}$$

$$\frac{P_1}{P_2} = \left(\frac{n_1}{n_2}\right)^3 \tag{2-5}$$

where n is a rotational speed, the subscript 1 denotes the original value and the subscript 2 denotes a new value.

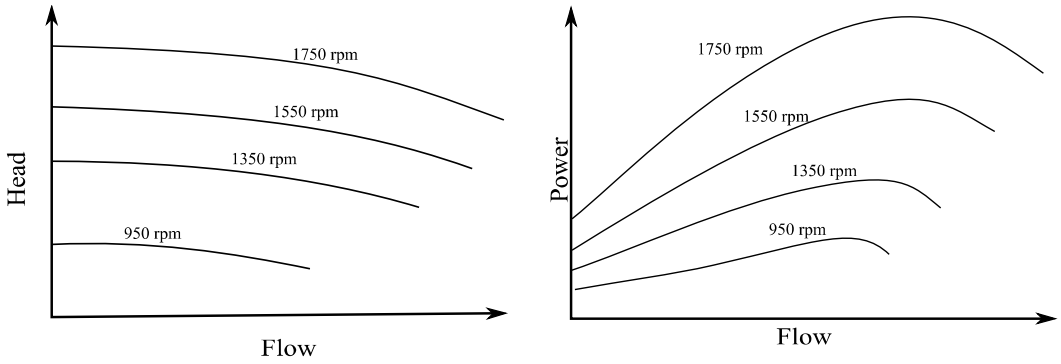

Figure 2-4 *QH* and *QP* curves of a pump for different rotational speeds.

2.1.4 Characteristic curves

A centrifugal pump that operates at a constant speed can deliver variable quantity of fluid from zero to the maximum value, depending on the total head. Typically, in the case of centrifugal pumps, the flow rate provided by the pump decreases as the head increases, and the flow rate becomes zero when the head reaches its maximum value. Mechanical power required for work also varies within definite limits. Some power is needed even at zero flow rate to overcome friction. It is usual to plot head, power, efficiency and NPSH against flow capacity at a constant speed. Figure 2-5 shows a typical performance chart. The curve marked QH shows how the

head changes with the flow. The curve labeled HP shows consumed power at different flows. The curve labeled EFF shows the efficiency as a function of the flow rate. Usually performance chart also show the minimum head required at the suction nozzle of the pump to avoid cavitation. It is shown by the curve labeled NPSH.

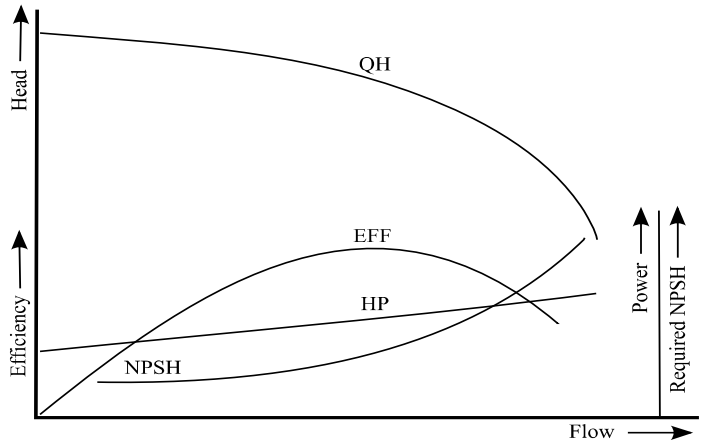

Figure 2-5 Typical performance chart.

In practice, curves are typically plotted for different impeller diameters when a pump operates at a constant speed. Figure 2-6 shows these curves for a Sulzer pump. The pump efficiency is shown with curves around the *QH* curve.

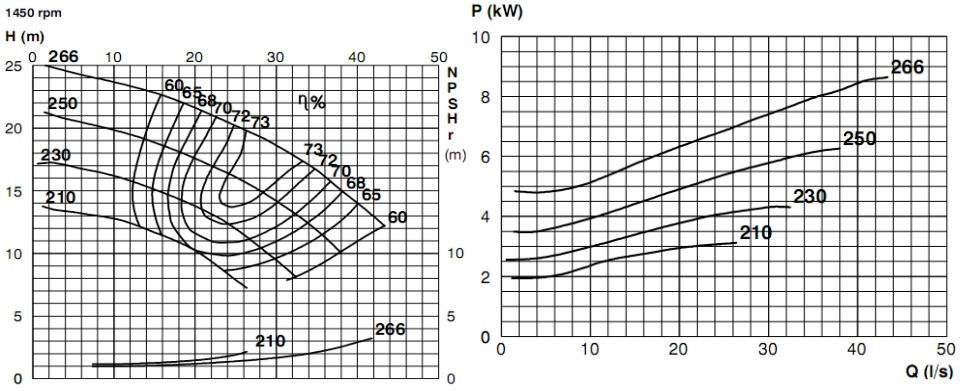

Figure 2-6 Characteristic curves for a Sulzer pump [8].

2.1.5 Process characteristics

A pump is located in a process, which often consists of valves and tanks. In general process characteristics can be presented with the static and dynamic head (Figure 2-7). Typically, static head is the vertical distance of fluid levels at the suction and discharge sides of the pump. It is independent of fluid flow rate. Dynamic head equals the effect of friction and is proportional to the square of the flow rate. Pump operating point location is determined by the pump and process *QH* curves, and the pump operates in their intersection.

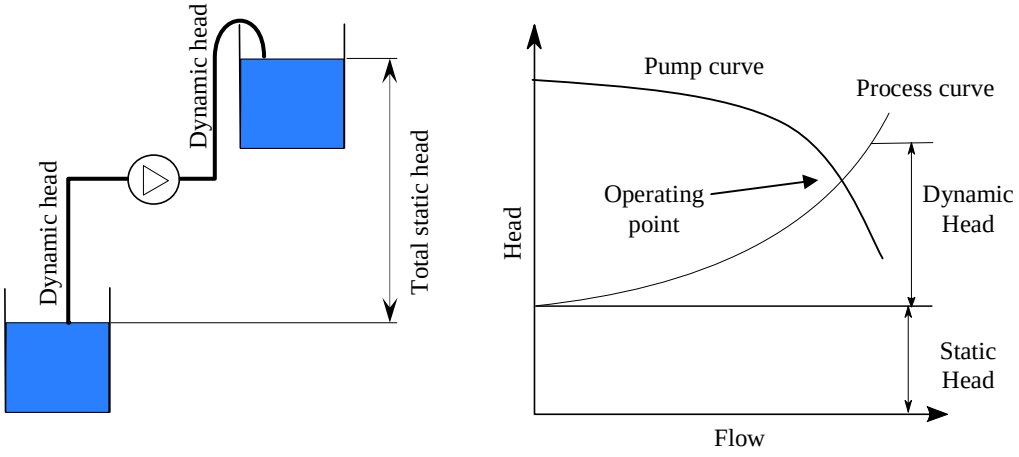

Figure 2-7 Static and dynamic head of a pump.

2.2. Induction motor

Induction motors are the most popular electric motor type in industrial applications nowadays. The reason is their reasonable price, low maintenance costs and good reliability. Typically, three phase induction motors are used. In Figure 2-8 an industrial three-phase induction motor from ABB is illustrated.

Figure 2-8 Typical industrial induction motor. [9]

2.2.1 Principles of operation

Induction motor consists of a rotor and a stator (Figure 2-9). Stator is a stationary part of a machine. It has individual windings for each phase. The stator can create rotating magnetic field. The most frequent type of stator winding arrangement is 3-phase. Among others, number of windings is dependant on number of pole pairs p used for each phase. The rotational speed of magnetic field, which equals motor synchronous speed n_s, is dependant on the power supply frequency f and the number of pole pairs.

$$n_s = \frac{f}{p} \cdot 60 \qquad (2\text{-}6)$$

So for f = 50Hz and p = 2, the synchronous speed will be 1500 rpm.

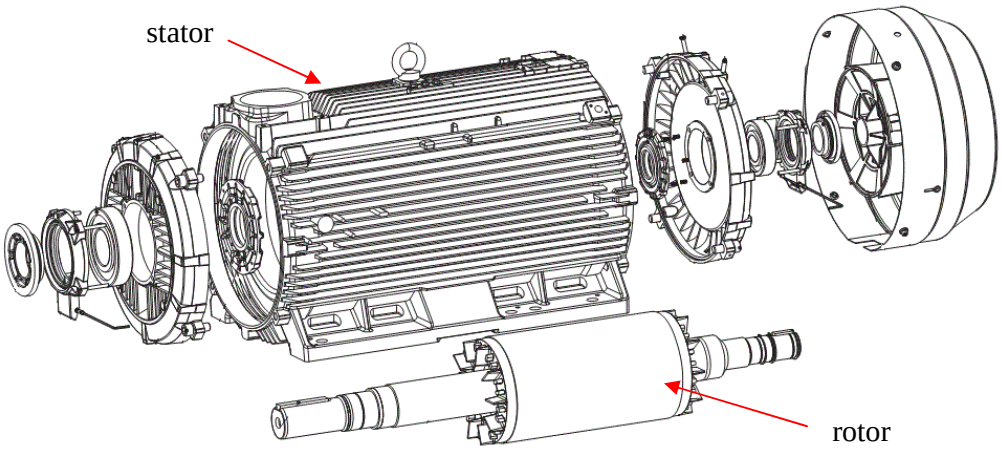

Figure 2-9 Typical structure of induction motor. [9]

Rotor is a non-stationary part of the machine. In induction motors three types of rotors are used: squirrel-cage, slip ring and solid core rotor. Squirrel-cage rotor is the most common type used. It is made up of bars of aluminum or copper that are connected at both ends by shorting rings. The core of the rotor is build of stacks of electrical steel laminations.

The stator creates a rotating magnetic field with its winding. This changing field penetrates the rotor bars and induces current in the rotor conductors. These currents interact with the magnetic field created by the stator which causes rotation of the rotor. Since there must be a phase difference between stator, and rotor magnetic field, the rotational speed of the rotor should be smaller than the rotational speed of magnetic field. This leads to a very important parameter of an induction motor – the slip *s*

$$s = \frac{n_s - n_r}{n_s}, \qquad (2\text{-}7)$$

where n_s is the rotational speed of the magnetic field created by the stator, n_r is the rotational speed of the rotor.

The Figure 2-10 shows the relation between slip and produced torque in induction motor. It shows that the rotational speed of induction motor changes with the change of the load. Thus the rotational speed of the induction motor can be predicted only, if the exact value of load is known.

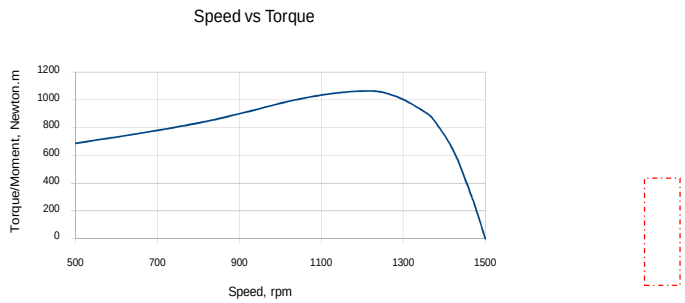

Figure 2-10 Speed vs Torque chart for an induction motor. The dashed rectangle denotes the operational region.

2.2.2 Speed control techniques

To adjust the rotational speed of an induction motor, the frequency of power supply should be adjusted. That can be easily done with a frequency converter. With the development of power electronics, a lot of frequency converters has had appeared in the market. The Figure 2-11 shows a typical frequency converter and its control panel from ABB. Parameters of a motor such as speed, current etc can be easily monitored and adjusted with the converter.

Figure 2-11 Frequency converter from ABB.

3. ESTIMATION OF ROTATIONAL SPEED

Rotational speed of a machine can be measured with portable devices that are based on mechanical and optical methods.. Their disadvantage is the need of direct access to the rotating shaft. Usually all rotating shafts are covered with a protective casing, like in Figure 3-1, which prevents the use of the handheld devices for rotational speed measurements. In this chapter, the use of vibration measurement in the estimation of pump drive rotational speed is discussed.

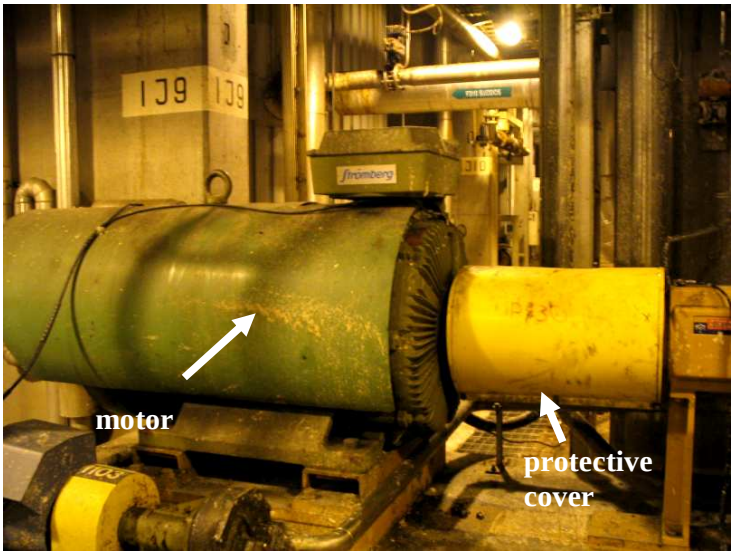

Figure 3-1 Industrial pump drive installation in a paper mill.

3.1. Vibration measurement

Vibration analysis is a proven technique to monitor the condition of equipment. All rotating machines produce vibrations that are a function of the machine dynamics, such as the alignment and balance of rotating parts. Vibration analysis can provide valuable information about the accuracy of shaft alignment and balance, the condition of bearings or gears, and the effect of resonance from the housings, piping and other structures on the machine.

A vibration analysis system usually consists of four basic parts:

1. Signal pickup, also called transducer;

2. A signal acquisition hardware;

3. Analysis software;

4. A computer for data analysis and storage. [10]

In this work a vibration analysis is utilized to determine the pump rotational speed. The frequencies that can be found in vibration spectrum of a pump drive will be explained in the following sections.

3.2. Vibration sources in electrical drives

Vibrations in an induction motor can be divided in two groups according to their nature: magnetic and mechanical. In the induction motor the torque is produced by forces that are applied to radial sides of the rotor. When these forces are not balanced, vibration occurs in the motor. Main reasons of unbalance of forces are current and airgap variations. [11]

Current variations can occur due to rotor or stator faults. Stator fault is a shortening in stator windings. This fault introduces vibration components at a 2*line frequency. Rotor fault means broken rotor bars. This kind of fault introduces vibration components at the frequency of rotational speed (1*rpm) with sidebands at 2*slip frequency around the 1*rotational frequency. Slip frequency s is

$$s = \frac{f_r}{f_s}, \qquad (3\text{-}1)$$

where f_r is the rotational frequency of the rotor and f_s is the rotational frequency of the magnetic field. Later, the 1*rotational speed frequency is referred as 1*rpm.

Airgap variations are caused by the eccentricity, and they lead to variations in the magnetic reluctance. According to the Equation 3-2, it can be seen that the variation in

reluctance causes the variation in flux. That will cause current variations and consequently the forces that act on the rotor will become unbalanced.

$$F = \frac{MMF}{R_m}, \qquad (3\text{-}2)$$

where F is the flux, MMF is magneto motive force and R_m is total magnetic reluctance.[11]

Two types of eccentricity are known – static and dynamic. Static eccentricity is when the rotor revolves around its axis but the axis is shifted with respect to stator axis by some value [12] (e.g. because of bearing wear or misshapen stator). It produces vibration components at 2*line frequency. Dynamic eccentricity corresponds to the case when, compared with the static eccentricity, symmetrical location of the rotor axis changes during the rotation of the rotor [12] (e.g. because of rotor bow). It produces vibration components at 1*rpm and 2*slip frequency sidebands about a center frequency of 1*rpm.[11]

Consequently magnetic sources of vibration can be divided to “rotating” and “stationary” problems according to vibrations they produce. Table 3-1 gives the presentation of the origins of magnetic vibrations.

Table 3-1 Typical causes of vibration in induction motors [11].

Type of problem	**Frequency of vibration**	**Typical cause**	
		Air-gap variations	**Current variations**
Stationary	2* line frequency	Static eccentricity, weakness of stator support	Stator winding faults
Rotating	1*rpm with 2*slip frequency sidebands	Dynamic eccentricity Loose rotor bars	Broken or cracked rotor bars, or shorted rotor lamination

Another kind of vibrations in an induction motor has a mechanical nature. They are caused by faults occurring in a rotating shaft. Most common shaft vibrations are presented in the Table 3-2. It's obvious that 1*rpm is the main vibration component and it can be caused by different fault conditions. To localize vibration problem frequency components evaluation is needed. For example misalignment and bent shafts produce large component at 2*rpm, while unbalance doesn't have that component. If there is a spatial truncation in vibrating system, then it appears as a high number of harmonics in vibration frequency spectrum. Components caused by bearing failures are dependent on the bearing type. In rolling element bearings local faults can produce vibration components with resonances between 1kHz to 20kHz, while sleeve type bearings give components at a fraction (0.43 to 0.48) of the rotational frequency.

Table 3-2 Characteristic frequencies of vibration in induction motors [11].

Type of problem	Dominant frequency	Dominant plane
Unbalance	1*rpm	Radial
Bent shaft or misalignment (angular)	1*rpm, 2*rpm [1]	Axial
Misalignment (parallel)	1*rpm, 2*rpm [1]	Radial
Mechanical looseness	1*rpm, 2*rpm [2]	Radial
Bearings failure	(0.43÷0.48)*rpm	Radial

[1] – high 2x component can be expected;
[2] – high harmonics and inter harmonics;

3.3. Vibration sources in pumps.

In every pump type dynamic forces of mechanical and hydraulic origin are present so a certain vibration is present in the pump operation. The most typical component is the vane passing frequency (VPF).

The source of VPF is a pressure fluctuation as a vane passes a discontinuity within its chamber. This discontinuity is usually the edge of the discharge opening. The VPF is always a product of rotational speed and the number of vanes.

Besides the normal pump operation, vibration may be caused by the unbalance, misalignment, mechanical looseness, base installation, cavitations, etc. Mechanical unbalance is the most common cause of vibration in rotating machinery. In linear

systems it produces frequency equal to the rotational speed of the pump (i.e., 1*rpm). An unbalance can be caused by errors in design, manufacture, assembly, initial balancing or by the impeller damage. A hydraulic unbalance is induced by fluid flow and usually caused by poor suction side piping arrangement. A flow restriction close to the pump suction causes fluid to have different speeds within the pipe. If the flow will have different speed when reaching the impeller, the dynamic unbalance will impose a high radial vibration at the rotational frequency. Misalignment is a second major reason. It occurs when centerlines of two rotating shafts have difference in offsets or angles. Misalignment usually produces vibration components at 1*rpm, 2*rpm and sometimes at 3*rpm.

Table 3-3 Typical causes of vibration in pumps and characteristic frequencies.

Fault	Frequency	Remarks
Unbalance	1*rpm	Most common cause of vibration
Misalignment of couplings or bearings. Bent shaft.	1*rpm and 2*rpm	Appearance of axial vibration.
Shaft looseness	Many rpm harmonics	Usually accompanied by unbalance and/or misalignment.
Hydraulic forces	Vane passing frequency	
Rubbing	1*rpm with higher harmonics	Usually occur if shaft is bent or bearings worn
Cavitations	Wide frequency noise	Can also increase hydraulic forces on the impeller -> rise of VPF

3.4. Frequency-domain analysis of the measured vibration

The transducer used in vibration measurement produces a voltage output. To determine the frequency content of the measured and stored signal several methods can be applied. In this work the following two methods are evaluated: a fast Fourier transform and a Goertzel algorithm.

3.4.1 Fast Fourier transform

Fourier transformation is a well known algorithm. It comes from the study of Fourier series. Fourier series are the series of simple waves (mathematically represented by sinus and cosines) which allow the representation of complicated periodic functions. Fourier transform deals with continuous signals but in our case the vibration data is discretized by data acquisition card. For this reason, the discrete Fourier transform (DFT) can be used to analyze the frequency content. The DFT is defined as follows

$$X_k = \sum_{n=0}^{N-1} x_n \cdot e^{-\frac{2\pi i}{N} kn}, \; k=0,\ldots,N-1 \qquad (3\text{-}3)$$

where x_n is input signal, i is an imaginary unit, $e^{-\frac{2\pi i}{N}}$ is a primitive N'th root of unity and X_k is the representation of amplitude and phase of the different sinusoidal components of the input signal x_n.[13]

To speed up the computational process a modified version of Fourier transform is used – fast Fourier transform. It is an efficient algorithm to compute the discrete Fourier transform. Evaluation of DFT definition directly requires order of N^2 operations: there are N outputs X_k, and each output requires a sum of N terms. FFT method requires order of N*log(N) operations to compute the same results. Thanks to this fact FFT is widely used in signal processing today. For example there is a special module (VI) in LabVIEW development environment by National Instruments that can compute the FFT of any input signal.

3.4.2 Goertzel algorithm

The Goertzel algorithm is a digital signal processing technique for identifying frequency components of a signal, published by Dr. Gerald Goertzel in 1958. While the general Fast Fourier transform (FFT) algorithm computes evenly across the bandwidth of the incoming signal, the Goertzel algorithm looks at specific, predetermined frequencies. [14]

A practical application of this algorithm is recognition of the DTMF tones produced by the buttons pushed on a telephone keypad. [14]

The Goertzel algorithm requires several parameters to be defined before actual computation. These are sampling rate and block size. Sampling rate should be selected according to Nyquist rule: the sampling rate will have to be at least twice the frequency of interest. Block size parameter controls the frequency resolution. After the parameters are selected several constants needed to be computed in accordance with next equations.

$$\begin{aligned} k &= \left(0.5 + \frac{N * target\_freq}{sample\_rate} \right) \\ \omega &= \frac{2*\pi}{N} * k \\ \text{cosine} &= \cos\omega \\ \text{sine} &= \sin\ \omega \\ coeff &= 2 * \text{cosine} \end{aligned} \qquad \text{(3-4) [15]}$$

where N is the block size, and *target_frequency* is analyzed frequency.

Next the actual computations follow. They require three variables: Q_0, Q_1, Q_2. Q_1 is used to store previous value of Q_0. Q_2 is used to store the value of Q_0 two times ago. Q_2 and Q_1 are initialized with zero value. Next the sequence of equations (3-5) is computed in a cycle. The number of cycle iterations is equal to the block size.

$$\begin{aligned} Q_0 &= coeff * Q_1 - Q_2 + sample \\ Q_2 &= Q_1 \\ Q_1 &= Q_0 \end{aligned} \quad , \qquad \text{(3-5) [15]}$$

where *sample* is a sample of time-domain data. Next sample is acquired after each iteration. After the cycle is finished parameters of the analyzed frequency can be obtained by employing next equations sequence.

$$\begin{aligned} real &= (Q_1 - Q_2 * cosine) \\ imag &= (Q_2 * sine) \\ magnitude^2 &= real^2 + imag^2 \end{aligned} \quad , \qquad (3\text{-}6)\ [15]$$

where *real* is the real part of frequency amplitude, *imag* is imaginary part of frequency amplitude.

Although the Goertzel algorithm is oriented to tone detection, one can use it for the spectrum analysis by looking at multiple tones to create a spectrum. That is exactly how it is utilized in this project. Frequency sweep across the spectrum of interest is done to determine the vibration spectrum and then peaks in the output denote vibration components. This method is acceptable for narrow frequency ranges.

3.5. Conclusion

This chapter presented the clear definition of characteristic frequencies that can be found in pump drives. The major one (with the highest amplitude) is the shaft rotation frequency. For a typical drive with the rotational speed of 1500 rpm it will be 25 Hz. Also harmonics are often present in the spectrum. For the previous example they are located at 50, 100, 150 Hz. Another peculiar frequency is the vane passing frequency. If the pump vane number is known it could be used in the estimation. However, it is not usually printed on the pump nameplate.

These estimations help to define the transducer's frequency rage. In general the vane number can be assumed to be less than eight. For the case of 3000 rpm drive a transducer with frequency range up to 400 Hz is needed to get all the relevant data during measurements.

4. IMPLEMENTATION OF THE MEASUREMENT SYSTEM

In this chapter, an overview of available platforms for the project is presented. Next, the requirements for the project are outlined and the selected platform (hardware and software parts) is described in detail. After this, the created software solution is presented. All the created components are depicted.

4.1. Applicable hardware approaches for the measurement system

There are a lot of different platforms nowadays that can be used for a measurement device. In the following sections embedded systems platforms and personal computer platform are introduced.

4.1.1 Embedded systems

Embedded systems today are very popular. The main component of such systems is microcontroller or microprocessor. There is a huge variety of these components, but they can be categorized by data bit width, instruction set and purpose.

According to **data bit width** there are 8 bit, 16 bit and 32 bit architectures. The main difference is the highest number processor can represent. The complexity of architecture increases the performance and the price of the processor.

According to **instruction set**, processors can be either reduced instruction set computer (RISC) or complex instruction set computer (CISC). The majority of embedded systems are based on RISC processors. The most popular among them have an Advanced RISC Machine (ARM) architecture.

Processors can be divided to general purpose and special purpose groups according to their **designed usage**. The difference is usually how many peripheral devices are included in a processor.

The selection of the processor type for the project is based on the required solving power, support for external devices, ease of development of hardware and software.

The next step is the selection of hardware platform for the device. The device can be created from a scratch or an existing hardware platform can be used. The example of available hardware platform is commercial handheld devices. If you select such device as your hardware platform – the only problems left are to find a way to connect needed sensors and to write software that handles processing algorithm. Another way is to develop platform from scratch using demo board provided by a processor manufacturer. Advantage of this way is that only needed hardware parts are used. The main drawback of this approach is longer development as the hardware must be designed from a scratch.

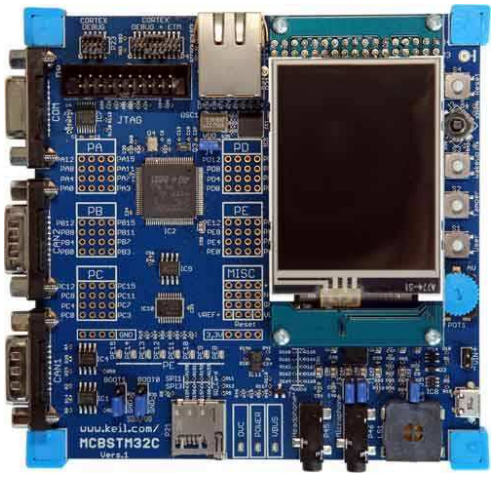

Figure 4-1 Demo board with ARM microprocessor. These boards are mainly used for development of software part of a project. The hardware part can be copied from a demo board design with the exclusion of unneeded components.

4.1.2 Personal computers

PC is a general purpose computer. The most common processors used in PC are x86-compatible CPUs. According to size PC can be divided to portable (laptop) and desktop computers. Laptops are mobile, they usually have battery so they can operate without an external power supply. There is a high variety of peripheral devices developed for PC. For example National Instruments has created different data acquisition devices.

There are many different development environments that can be used with a PC. Among them are Visual Studio from Microsoft, LabVIEW from National Instruments, Delphi from Borland (Figure 4-2).

Figure 4-2 Laptop running NI LabVIEW software and NI data acquisition card connected.

The usage of PC platform can sufficiently reduce development time. This is thanks to wide spread of PC, high number of available peripheral devices and different development environments.

4.2. Requirements for the system

Before the actual system platform is selected the requirements for this platform should be stated. The future platform should:

- provide effective tools for software development;
- be portable;
- be capable of storing results of measurements;
- provide easy ways to transfer acquired results to files;
- provide means for the data visualization;
- be able to work without external power supply;
- provide easy ways to acquire data from a sensor.

The only platform that suits all the posted requirements and provides a small development time is a mobile personal computer. There is a high variety of development tools and peripheral devices for measurement available for this platform. There are also models of mobile computers that are specially designed to operate in hazardous industrial environment.

4.3. Platform of the project

4.3.1 Hardware platform

As was stated in the previous section, the only platform that suits all the requirements is mobile personal computer. The laptop selected for this project is Acer Aspire 2010 model (Figure 4-3). Its parameters can be found in Appendix 1.

Figure 4-3 Acer Aspire 2010 laptop running LabVIEW.

For a sampling device a data acquisition card from National Instruments was selected. Card model is NI USB-6009. Figure 4-4 presents the picture of DAQ card.

Figure 4-4 NI USB-6009 DAQ Card.

The DAQ card has four data acquisition inputs and can provide sampling rate up to 48 kHz with the resolution of 14 bits. Maximum voltage range for measurements is ± 10V. The card can also provide 5V output. Other parameters are presented in Appendix 2.

An accelerometer is used as a vibration sensor. As was stated in Chapter 3, the required frequency range of the transducer should be from 10 Hz to 400Hz. This allows the use of MEMS sensor for the platform as this sensor type has a limited bandwidth compared to piezo-electrical acceleration sensors. The main benefits of this type of sensors are:

- small size;
- DC voltage supply;
- voltage output for measured acceleration.

A transducer should also provide an easy way for mounting it on a pump drive, which prefers the use of a square formed acceleration sensor. According to these requirements an accelerometer model SCA111 from VTI was selected for this application. Its characteristics are presented in Appendix 3.

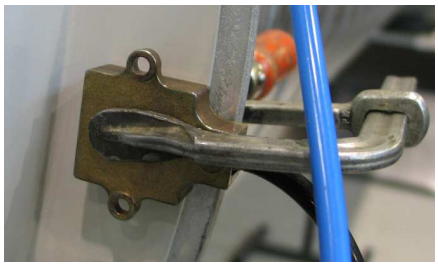

Figure 4-5 VTI SCA111-C12H1W accelerometer clamped to fan drive housing.

4.3.2 Software platform

There is a high variety of development environments for PC. For this project a LabVIEW development environment from National Instruments was selected. LabVIEW is a graphical programming environment for measurement, test, and control

systems development. LabVIEW offers integration with thousands of hardware devices and provides hundreds of built-in libraries for advanced analysis and data visualization. For this reason, LabVIEW is used in this mobile system project.

LabVIEW programs are called virtual instruments or VIs. Each instrument has a front panel (a user interface), a block diagram (a programming interface) and a connector panel (means for connecting Vis to each other). Programming in LabVIEW consists of placing VIs or other programmed elements on a block diagram and interconnecting them. Figure 4-6 represents the typical block diagram of a VI.

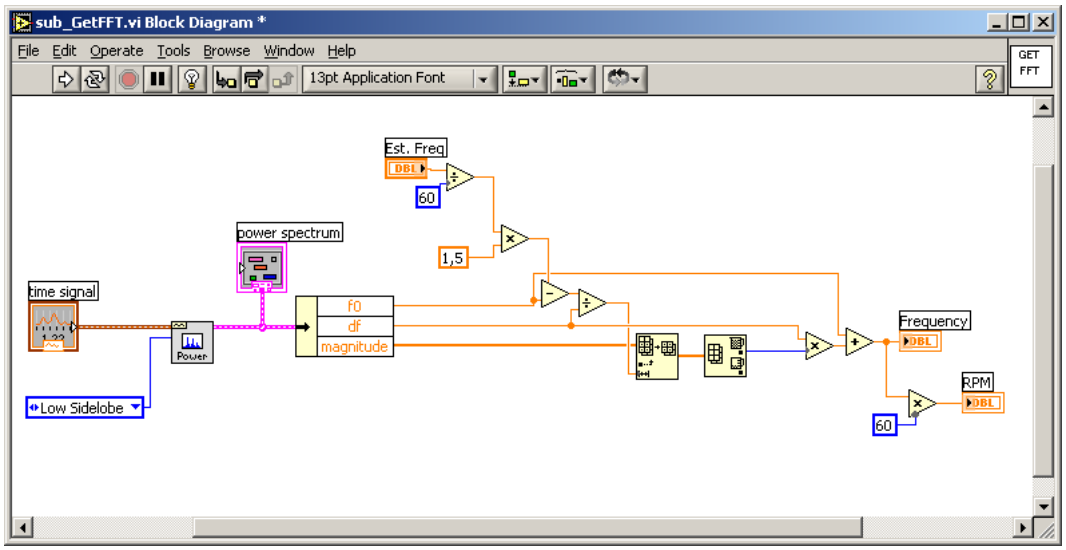

Figure 4-6 Block diagram of a VI.

VIs can be configured via their front panel. Figure 4-7 shows a front panel of a VI.

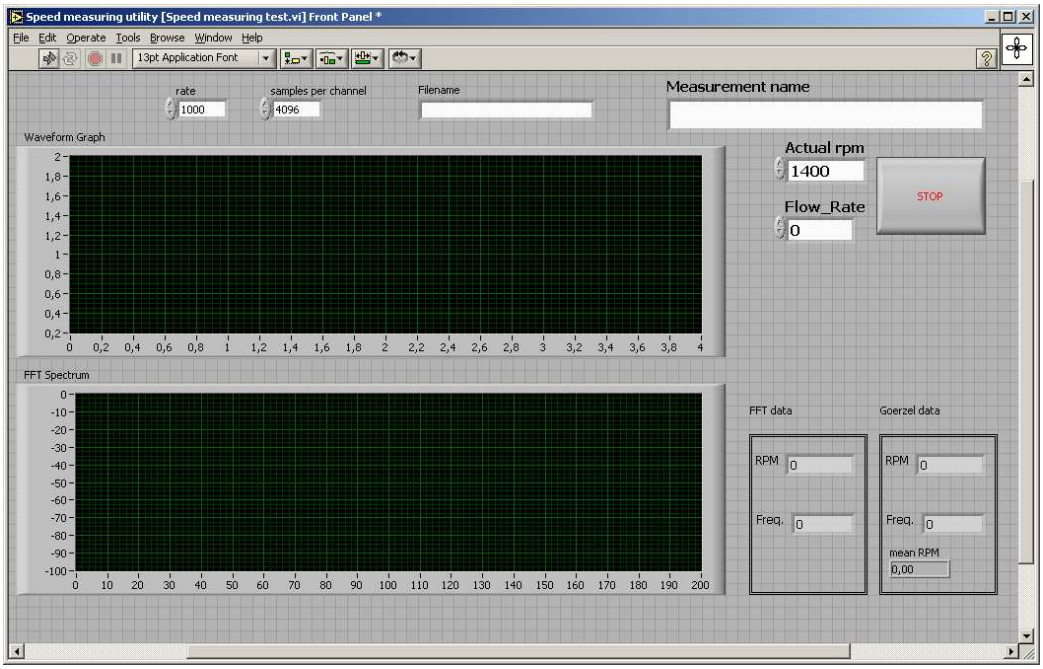

Figure 4-7 Front panel of a VI.

4.4. Description of the measurement system

The aim of the developed system is to give a handy tool for measuring the pump drive rotational speed and the resulting pump efficiency of the pump operating point location. The system should also provide easy ways for the storage of measured data and for later analysis. System must also have a friendly user interface.

The logical structure of operation is presented in Figure 4-8. According to this structure the program has four main parts: acquisition, analysis, store to database and output to screen.

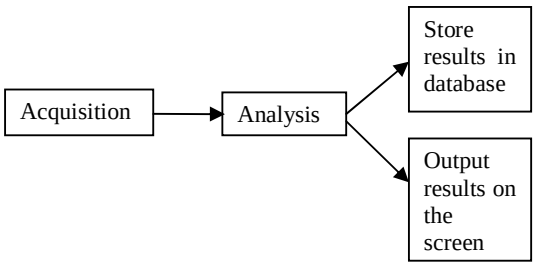

Figure 4-8 Logical structure of program operation.

4.4.1 Acquisition part

This part of the program provides the acquisition of the transducer output. This is done with the help of NI-DAQmx drivers. These drivers were created by National Instruments to support their data acquisition devices in the LabVIEW development environment. DAQmx provides an easy way to interact with a DAQ card.

The acquisition part of the program is presented only by one virtual instrument – **sub_GetDatafromDAQ**. This VI provides 4 seconds of sampled transducer data as an output. In normal use, there is no need to change its parameters. The front panel of the VI is presented in Figure 4-9 and block diagram in Figure 4-10.

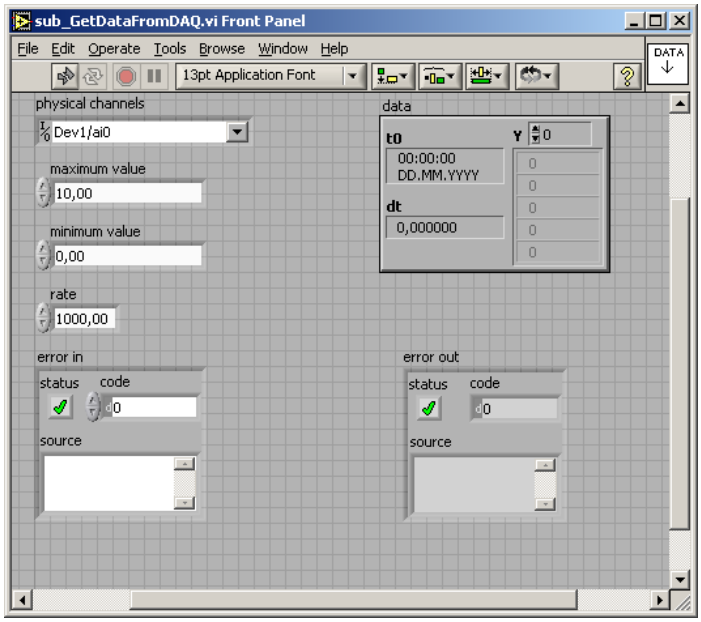

Figure 4-9 Front panel of sub_GetDatafromDAQ.vi.

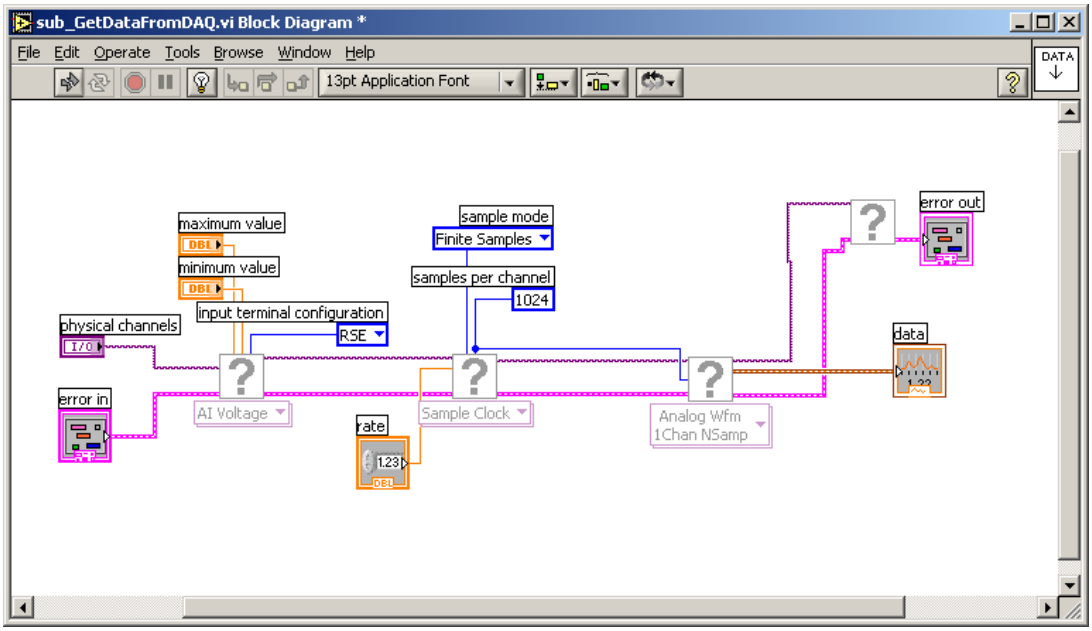

Figure 4-10 Block diagram of sub_GetDatafromDAQ.vi.

When the VI is called, it firstly creates a virtual channel for an acquisition card. At this step parameters of acquisition card are set up. These parameters are hardcoded into a VI but can be easily changed. Table 4-1 presents the list of these parameters and their default values.

Table 4-1 Virtual channel parameters.

Parameter	Description	Value
Physical channels	The list of physical channels that are for data acquisition	Dev1/ai0
Maximum value	Maximum input voltage	10
Minimum value	Minimum input voltage	0
Input terminal configuration	Configuration of input terminals	RSE (single ended, ground referenced)

If virtual channel initialization is correct, then DAQmx timing setup is called. This element sets the sampling parameters of data acquisition card. These parameters are configured for VTI sensor (to have four seconds of a measurement), but they can be easily changed. Default values are presented in Table 4-2.

Table 4-2 Sampling parameters.

Parameter	Description	Value
Sample mode	Sampling mode of data acquisition device. Can be continuous, finite or on demand.	Finite samples
Samples per channel	Number of samples returned after each read cycle	4096
Rate	Sampling rate	1000
Timing source	source of the timing signal	Sample clock

After successful completion of timing setup, a data read VI is called. This VI starts the sampling process and reads a block of sampled data. This element has only one parameter that tells how much data samples should be read. In this project the size of sampled data is predefined and is tied to the same property of the timing VI to provide four seconds of measurement. After acquisition process is completed, the sampled data block is returned to the "data" output connection of sub_GetDatafromDAQ VI and the virtual channel is terminated. After this the VI execution stops.

4.4.2 Analysis part

The most important part of this project is an analysis part. In this part the sampled data from transducer is analyzed for the presence of characteristic frequencies. The main idea of this part is to find rotational frequency component of a pump drive from the vibration spectrum. This is accomplished in two different ways: with the use of the fast Fourier transform and with the use of the Goertzel algorithm. In the Figure 4-11, a part of the main program is shown. In this part, the call to the two main components of the analysis part can be seen. These are **sub_Get_FFT** and **sub_Get_Goertzel**. It is also shown how the main program outputs the measured data to the front panel.

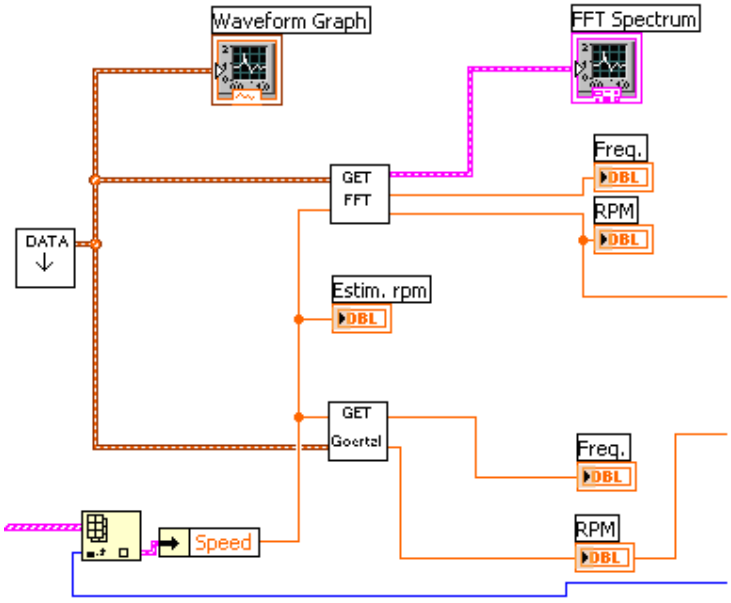

Figure 4-11 Part of the main program. The measurement part is conducted in VI marked "Data". After it the waveform is transferred to Get_FFT and Get_Goertzel VIs and a visualization graph. The value of estimated rotational speed is read from database (not shown) and also provided to VIs.

sub_Get_FFT VI uses fast Fourier transform to analyze sampled data for characteristic frequency. The front panel of this VI is shown in the Figure 4-12. The block diagram is presented in the Figure 4-13.

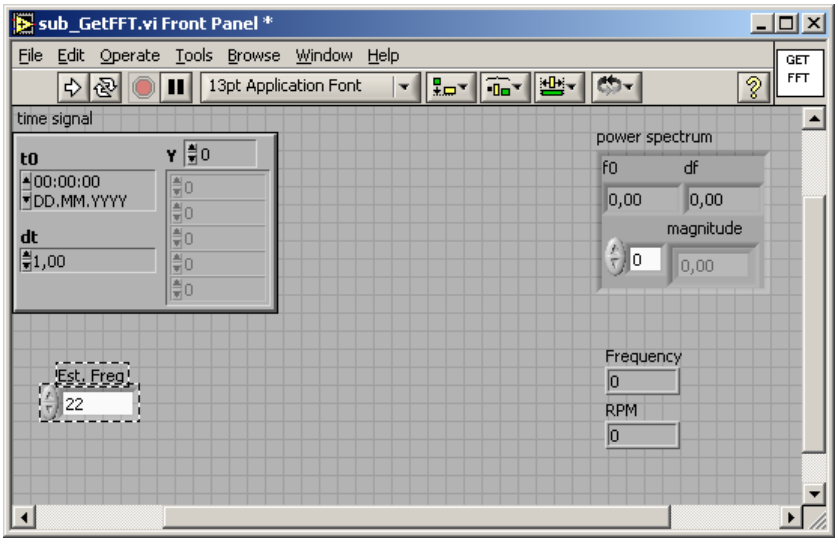

Figure 4-12 Front panel of sub_Get_FFT VI.

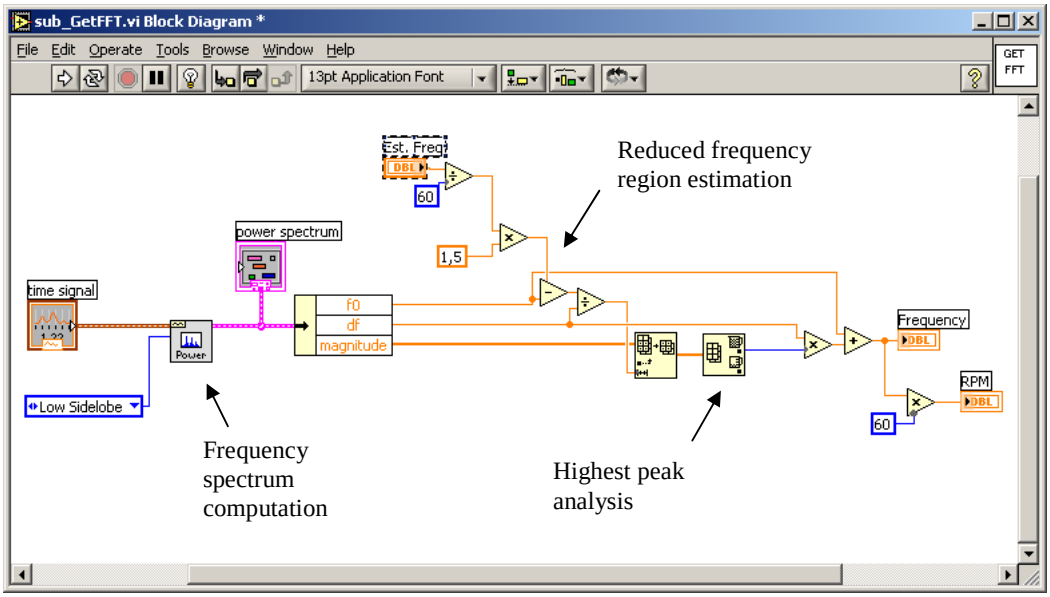

Figure 4-13 Block diagram of sub_GetFFT VI.

When this VI is called it has only two input parameters: “time signal” and “est. freq.”. “Time signal” is the sampled data from the data acquisition device. “Est. Freq.” is a roughly estimated rotational frequency of a pump drive. For instance, this value can be obtained from the motor or pump nameplate. After VI is called, the sampled data is fed to the Fast Fourier Transform Power Spectrum VI. This VI computes power spectrum of the input signal using FFT technique. The VI has several parameters but in

this case only one is used – time-domain window. This parameter is set to “Low Sidelobe”. This is done to reduce sidelobes of computed power spectrum values. After the computation is finished, the power spectrum data is transferred to the output connection “power spectrum” and also to the next stage of VI.

At the next stage, the frequency resolution parameter is used to compute the region of probable rotational frequency. The highest peak corresponding to the rotational speed will be searched. Using reduced frequency range helps to filter unwanted high frequency components that have high amplitude. Maximum value of the frequency range equals to “est. freq.” parameter multiplied by 1.5 and minimum value equals zero. Then, the reduced frequency region is analyzed for a highest peak using min max VI. After the highest peak is found its index is converted to frequency and frequency is converted to a rotational speed. The result of conversion is transferred to the “rpm” output connection of the VI.

sub_GetGoertzel VI works on the same principle – it evaluates a frequency spectrum created by Goertzel algorithm for the highest peak. The front panel of VI is presented in Figure 4-14. The block diagram is presented in Figure 4-15.

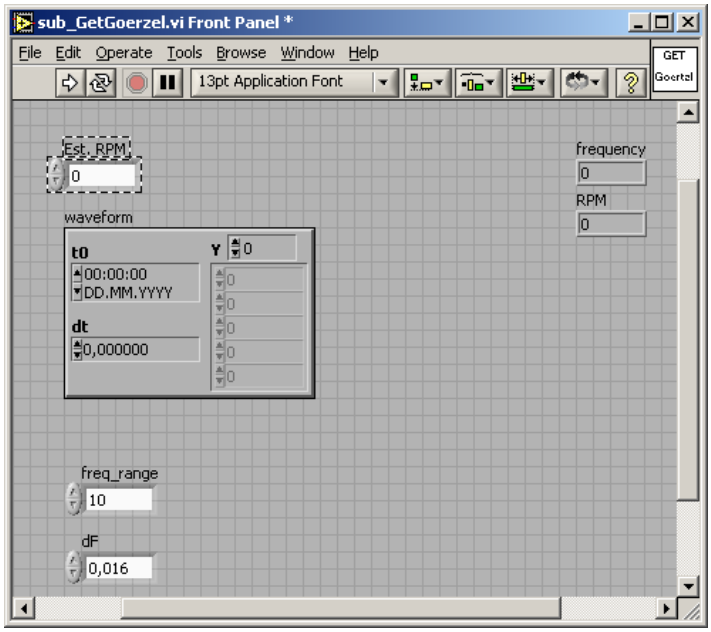

Figure 4-14 Front panel of sub_GetGoertzel VI.

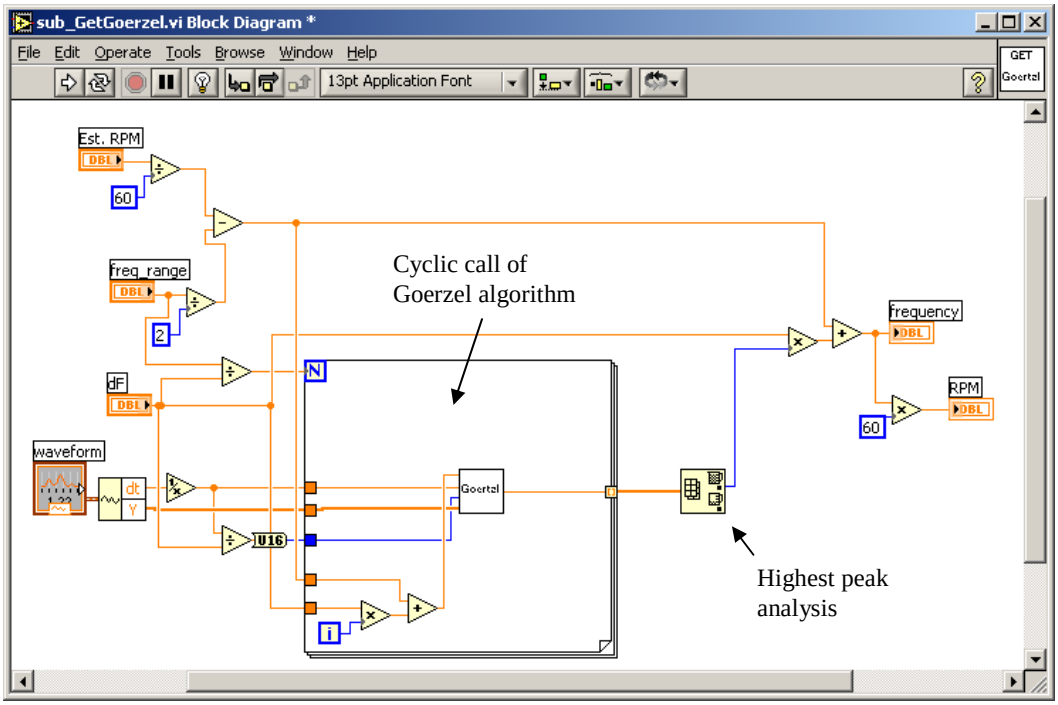

Figure 4-15 Block diagram of sub_GetGoertzel VI.

When this VI is called two parameters are passed: “waveform” and “est. rpm.”. “Waveform” is the sampled data from the data acquisition device. “Est. rpm.” is a roughly estimated rotational frequency of a pump drive. The VI also has two hardcoded parameters – “frequency range” and “dF”. “Frequency range” defines the size of the area of probable rotational frequency. This setting may affect the estimation results, if the roughly estimated rotational speed is strongly incorrect. “dF” defines the frequency resolution of the algorithm. The hardcoded values are 10 Hz for the “frequency region” and 0.016 for “dF”. Right after VI start-up values for the reduced frequency region are computed. Later they are used in a cyclic call of Goertzel algorithm VI that creates a frequency spectrum. The studied frequency range is now ±5 Hz around the initial guess for the rotational speed. Goertzel algorithm is realized by sub_Goerzel VI.

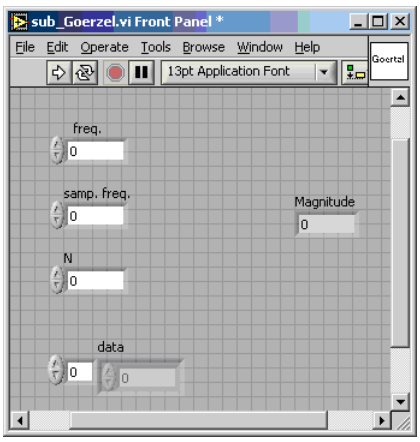

Figure 4-16 Front panel of sub_Goertzel VI.

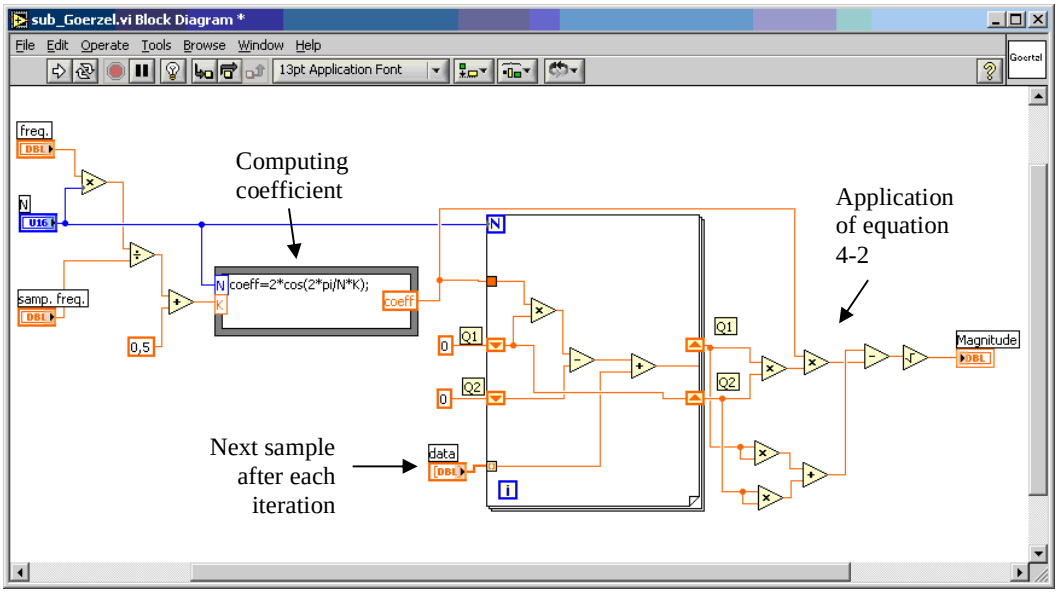

Figure 4-17 Block diagram of sub_Goertzel VI.

In **sub_Goertzel** VI an optimized version of Goertzel algorithm is used. The optimized Goertzel algorithm requires less computation than the basic one, at the expense of phase information. [15]

After VI is called several parameters are passed. They are “freq” – the frequency analyzed in current iteration of VI, “N” – number of sampled data points, “sampl. freq” – sampling frequency. Also the array of sampled data is passed. After “coeff” is computed the following equations sequence is run for every sampled data point.

$$Q_0 = coeff * Q_1 - Q_2 + sample$$
$$Q_2 = Q_1 \qquad (4\text{-}1)[15]$$
$$Q_1 = Q_0$$

After that the next equation is applied

$$magnitude^2 = Q_1^2 + Q_2^2 - Q_1 * Q_2 * coeff \qquad (4\text{-}2)[15]$$

and the result is passed to the “magnitude” output connection of the VI.

The result of cyclic call of sub_Goertzel VI is the array containing reduced frequency spectrum. This array is then analyzed for the highest peak. The index of found peak is converted to a frequency and then into a rotational speed. The result is passed to the “rpm” output connection of sub_GetGoertzel VI.

4.4.3 The database part

The database part of the program performs two actions: retrieves data from a database and stores data to a database. In this project an Access type of database was chosen. The reason for that is the convenience of data analysis and transfer. Access application from Microsoft is very popular these days. It is usually used for small and medium size databases. As an interface to an Access database a freely distributed LabSQL [16] package from Jary Travis Studios was used. This toolkit provides easy ways for accessing different types of databases from LabVIEW.

To ease the measurement process, a database with known electric motors and pumps was created. This database holds information about different parameters of pumps and motors. Figure 4-18 presents the screenshot of motor database section. Figure 4-19 presents screenshot of pump database section.

database4motor : Table

Type	Manufacturer	Speed	Power	Current	Cos Phi
4XUR328A2B3	Stromberg	1450	15000	30	0,86
LP100-125/130	Grundfos	2890	5500	11	0,87
M3BP160M	ABB	1465	11000	22	0,83

Figure 4-18 Motor section of database.

database4pump : Table

Type	Manufacturer	Speed	Imp Diameter	Blade	Char Q	Ch
APP22-80	Sulzer	1450	255	4	2.12,6.37,10.61,16.98,21.2,27.59,31.84,38.20,40.33	21.95,21.33,20.60,19.46,18
DC80/260	Serlachius	1485	250	5	13.25,17.52,21.44,24.57,28.05,30.69,34.70	21.86,20.85,19.73,18.55,16
LP100-125/130	Grundfos	2890	130	8	10,15.2,19.5,25.3,32.8,36.9	20.48,20.04,19.56,16.15,9.
P-X80X-1	Ahlström	740	755/665	6		

Figure 4-19 Pump section of database.

As can be seen, the pump section of the database holds the info about characteristic curves of different pumps. This information is required for the pump efficiency estimation.

The used toolkit provides an interface to Microsoft's ActiveX Data Objects (ADO). ADO is a set of Component Object Model (COM) objects providing access to different kinds of databases. Before actual usage the initial setup of ADO should be done. It can be done via ODBC Data source Administrator application (Figure 4-20) that can be found in Control Panel of Microsoft Windows. In this application an alias for the database should be provided. In the project the “MyDSN” alias is used. To change the alias or a path to the database a user should select “Configure” button in “System DSN” tab. In the new window shown in Figure 4-21 the alias and the path can be changed.

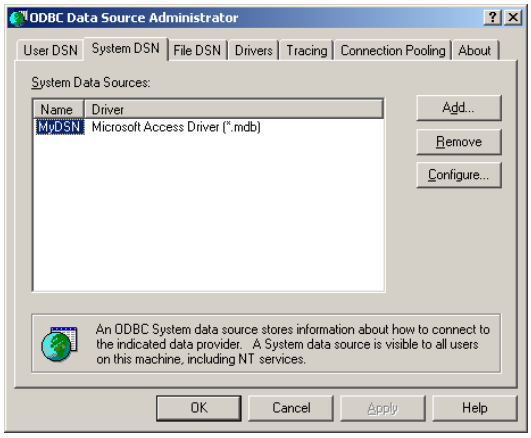

Figure 4-20 ODBC Data Source Administrator application window.

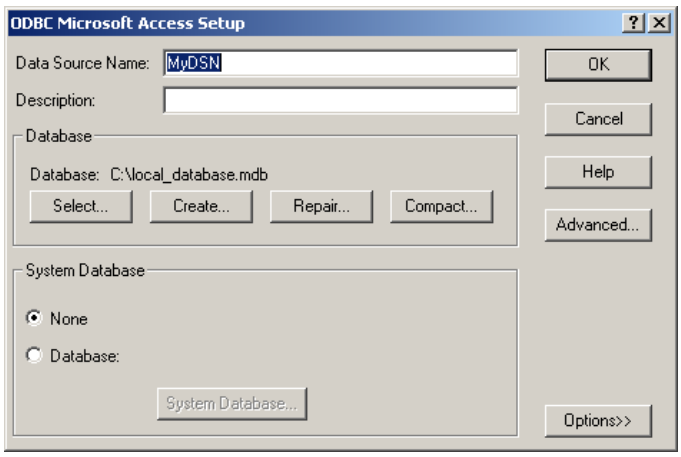

Figure 4-21 ODBC Microsoft Access Setup window.

Read from a database is done by **sub_ReadDatabase** VI. Front panel of the VI is presented in Figure 4-22. The block diagram is presented in Figure 4-23.

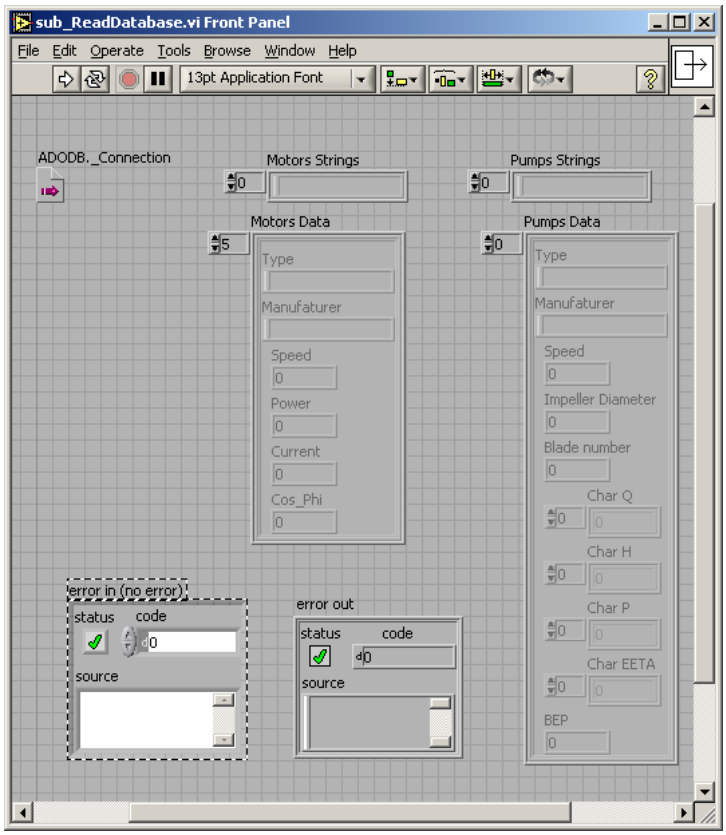

Figure 4-22 Front panel of sub_ReadDatabase VI.

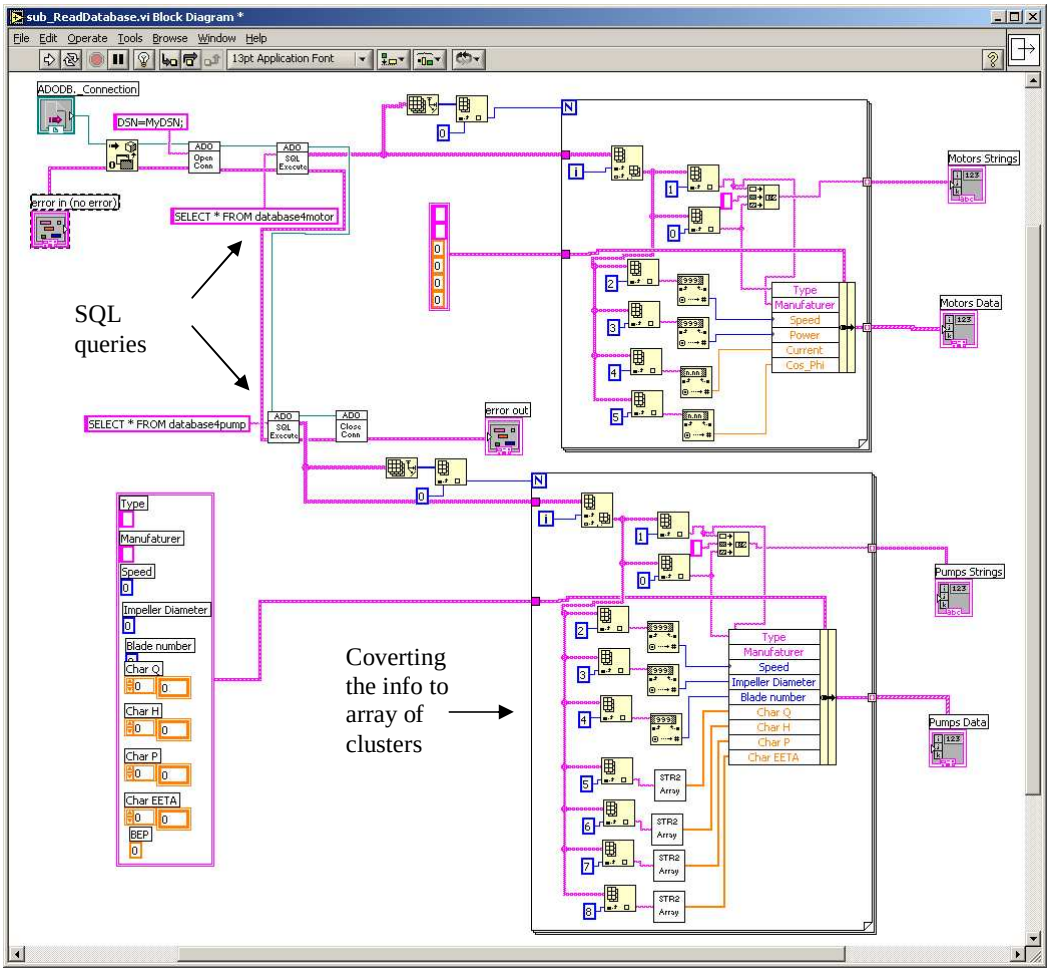

Figure 4-23 Block diagram of sub_ReadDatabase VI.

After **sub_ReadDatabase** VI is called it connects to an ADO server. After successful connection, a local database is opened. Then using Structured Query Language (SQL) query info about motors is read. This info is converted in the LabVIEW type cluster for more convenient usage. After this the SQL query is used to read the info about pumps and then the data is converted to an array of cluster type. After VI is completed the info about motors and pumps can be read from the outputs ("Motor Strings", "Motor Data", "Pump Strings", "Pump Data").

sub_Save2Database VI is used to save measured parameters to the database. It has the same principle of operation. Front panel of the VI is presented in Figure 4-24. The block diagram is presented in Figure 4-25. After VI is called the measured parameters are passed. Then after the connection to ADO server is created, VI opens

the database and using SQL queries writes all the parameters to the database. In the end it closes the connection to ADO server.

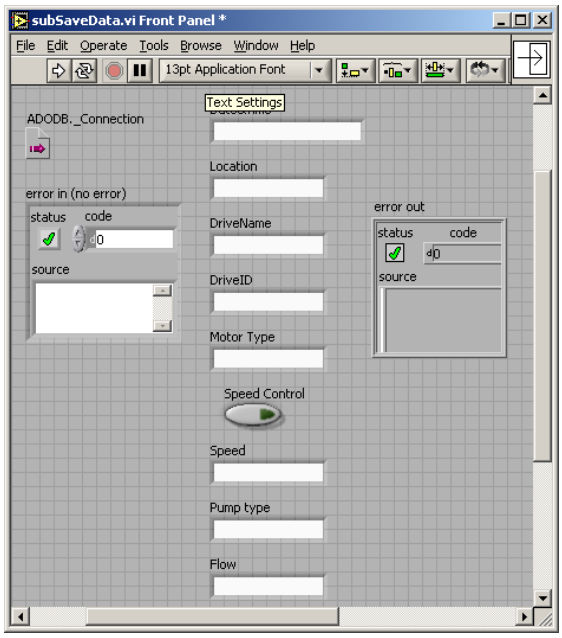

Figure 4-24 Front panel of sub_Save2Database.

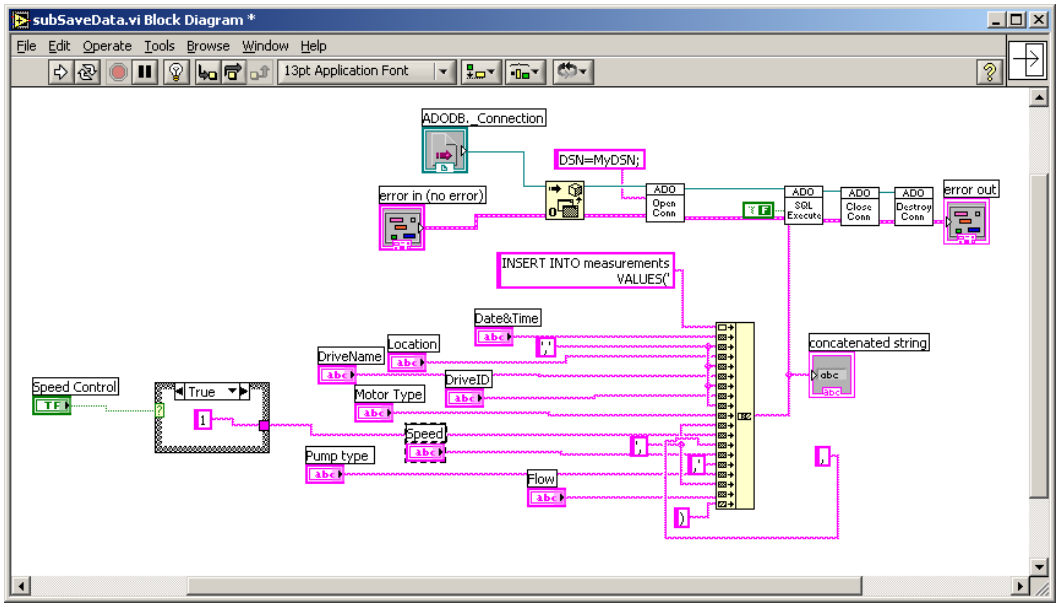

Figure 4-25 Block diagram of sub_Save2database.

4.4.4 Graphical user interface

Graphical user interface (GUI) is used for the user interaction with the program. The GUI is represented by the front panel of the program. It is presented in Figure 4-26.

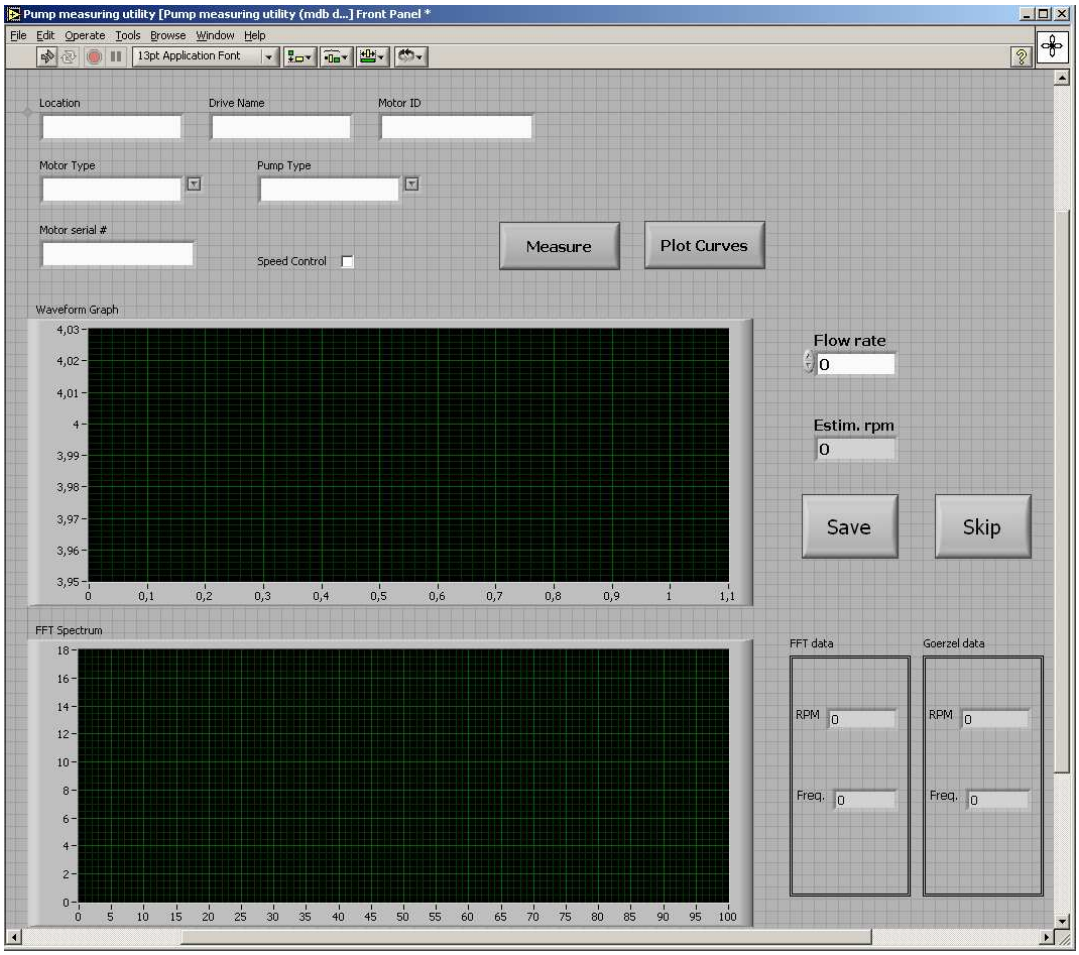

Figure 4-26 Front panel of the program.

The front panel has several input fields. These ones are needed to be filled before starting the measurements.

- Location – the place where measurements are conducted;
- Drive name – the name of the pump drive (e.g. “Water pump”);
- Motor ID – identification number of a drive (e.g. “#3”)

- Motor serial – serial number of a motor;
- Speed control – indicates if a motor has a speed control option;
- Flow rate – flow rate of the pump measured by a portable device;
- Motor type – manufacturer and model of a motor, is selected from database records (Figure 4-27)

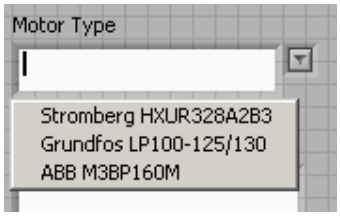

Figure 4-27 Example of motor type selection.

- Pump type – manufacturer and model of a pump, is selected from database records (Figure 4-28)

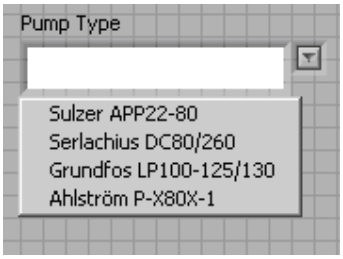

Figure 4-28 Example of pump type selection.

To start measurement process a user should select “Measure” button. After measurement process is finished the results are presented in several places. “Waveform graph” presents the waveform of sampled transducer signal. “FFT Spectrum” presents the FFT power spectrum of the acquired transducer signal. “FFT data” and “Goertzel data” frames shows the rotational speed and the rotational frequency computed by respective algorithms. After results are shown a user can either choose to save them by selecting button “Save” or skip them, by selecting button “Skip”. Also there is an

option to plot the measurement results on a characteristic curve. To employ this option a user must select “Plot curves” button. After selecting this button a new window is opened (Figure 4-29). This window presents a characteristic curve of a measured pump. This curve is adjusted for the measured rotational speed. Current working point of a pump is also plotted. It is in the intersection of a “flow” and “QH curve scaled” line. When the operating point is known, the respective efficiency can be determined from the pump efficiency curve. Consequently, the pump efficiency can be determined with the developed mobile system.

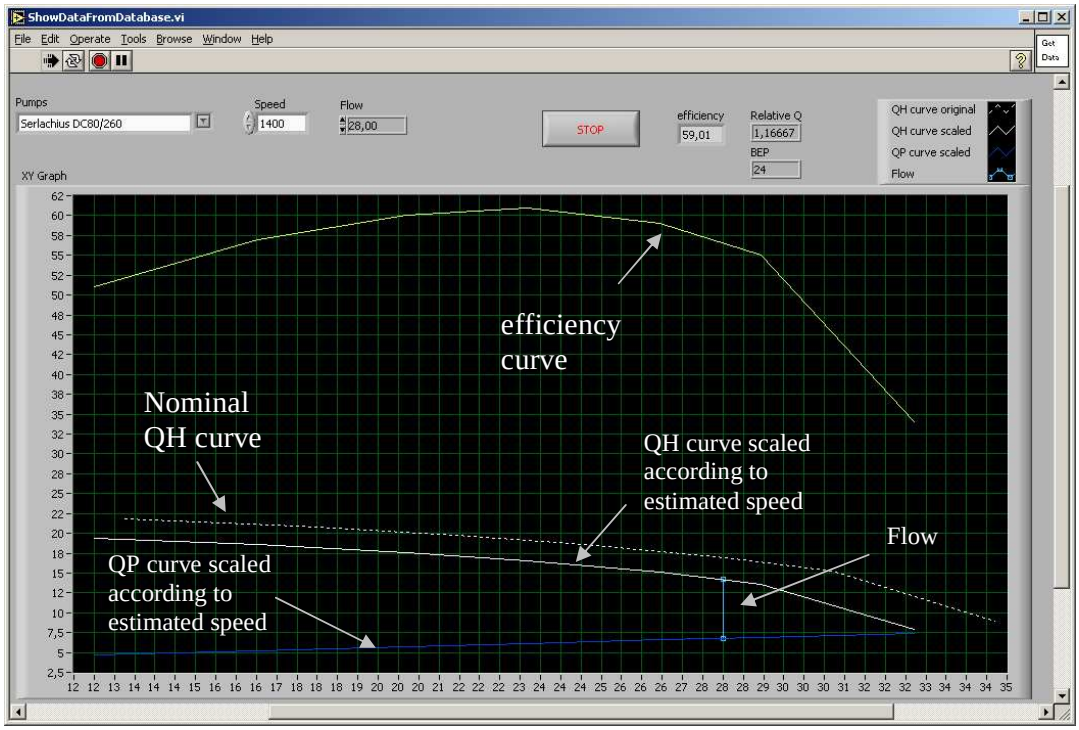

Figure 4-29 Front panel of characteristics curve window.

Block diagram of characteristic curve window is shown in the Figure 4-30.

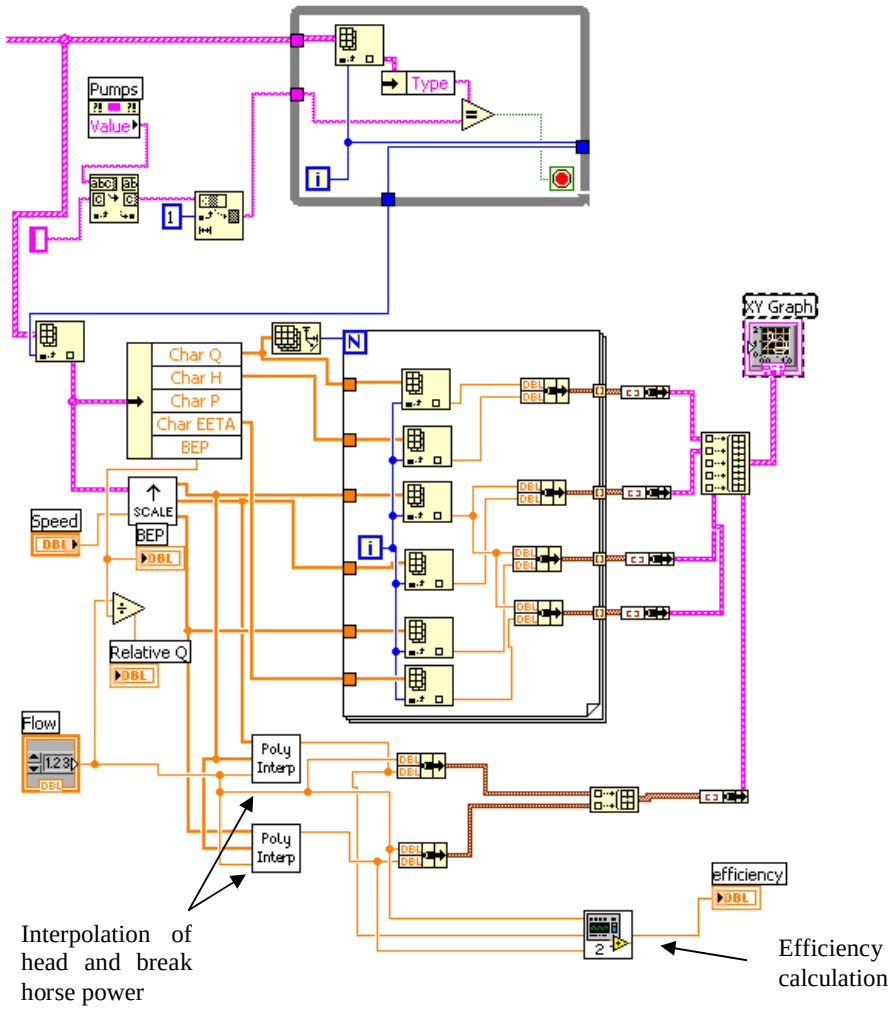

Figure 4-30 Block diagram of characteristic curve window VI.

The logical structure of the VI can be easily seen from the block diagram. After VI is called several parameters are passed. These are: array of clusters with information on pump parameters (from database), measured speed and measured flow. Pump characteristic curves are scaled in the SCALE VI according to affinity laws. The front panel of SCALE VI is presented in Figure 4-31. The block diagram of the VI is presented in Figure 4-32.

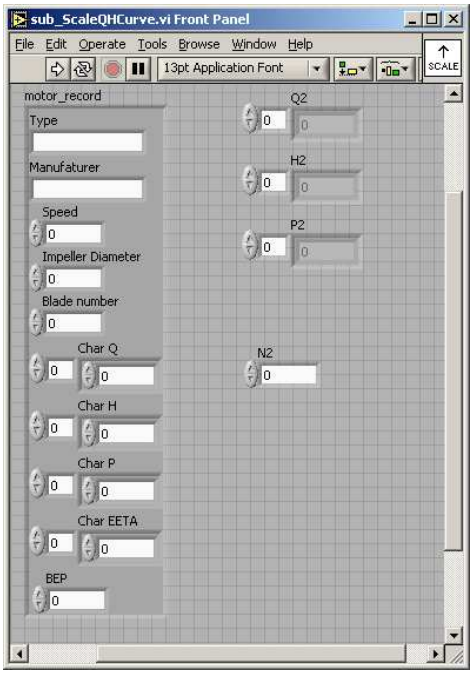

Figure 4-31 Front panel of SCALE VI.

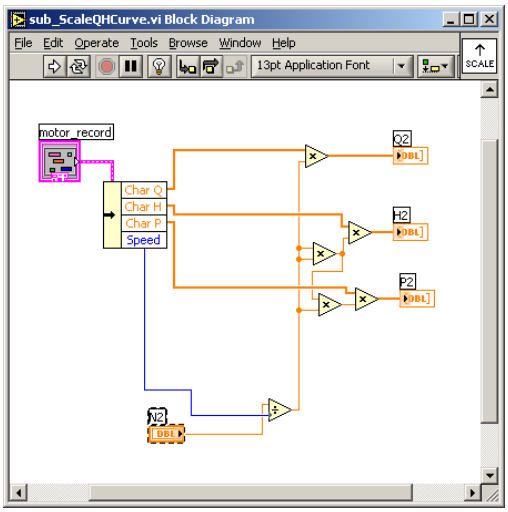

Figure 4-32 Block diagram of SCALE VI.

After characteristic curves are scaled they are plotted on the graph. The efficiency is calculated using polynomial interpolation of *QH* and *QP* curves in accordance to measured flow. The interpolated values are provided to **sub_efficiency** VI. The front panel and the block diagram of this VI are shown in the Figure 4-33. As it can be seen, this VI uses the Equation 2-2 for the calculation of the pump's

efficiency. The used value for fluid density is 998 kg/m^3 and the used value for the earth gravitation constant is 9.81 m/s^2. These values can be adjusted.

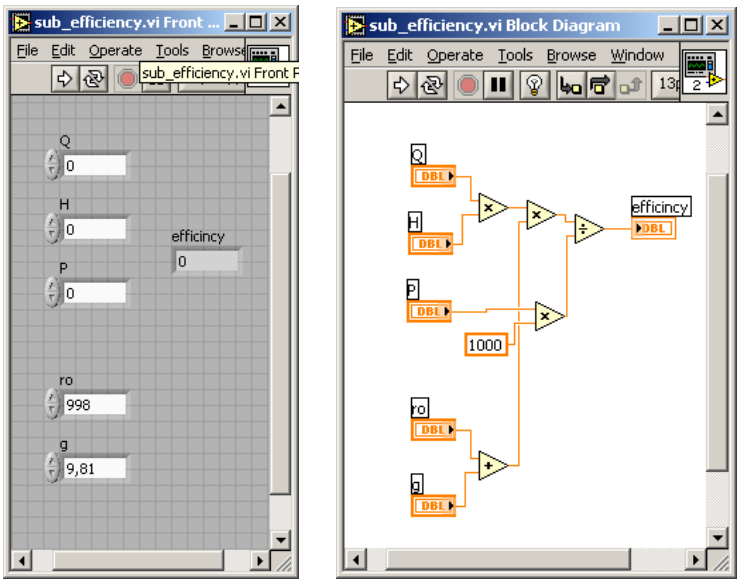

Figure 4-33 Front panel and block diagram of sub_efficiency VI.

5. LABORATORY EVALUATION

Measurements conducted with the created system are presented in this chapter. The main purpose of conducted measurements is to evaluate the system and check the correctness of results. Tests were carried out in Lappeenranta University of Technology. Three drives were measured: two pump drives and a fan drive. First pump drive was Sulzer APP22-80 pump equipped with an ABB induction motor. The second one was Serlachius DC80/260 pump driven by Stromberg induction motor. The fan drive was FläktWoods AXIPAL BZI VA630 4P driven by an ABB induction motor. All drives were controlled by an ABB ACS M1 frequency converter.

5.1. Measurement setup

Pump measurements were conducted in laboratory of pumps in Lappeenranta University of Technology. Following list of tools was used for the measurement process:

- Acer Aspire 2010 laptop
- NI USB-6009 DAQ card
- VTI SCA111-C12H1W accelerometer
- UNIFLOW 1010 ultrasonic flow rate meter
- Dataflex 22-100 torque and rotational speed metering coupling

The measurement program was installed on the laptop. Data card was used for acquisition of vibration signal from VTI sensor. UNIFLOW flow meter was used for measuring flow of the pump but as this is a non-portable device, a portable analog Omega F0613 was also tested during measurements. Dataflex metering coupling was used for the precise measurement of the rotational speed.

5.2. Test measurement with Sulzer pump drive

The measured Sulzer pump drive (Figure 5-1) consists of Sulzer APP 22-80 centrifugal pump and ABB M3BP160M4 induction motor. The rotational speed of the pump drive is controlled by ABB ACS M1 frequency converter.

Figure 5-1 Sulzer pump drive.

According to the nameplate, the motor nominal speed is 1460 rpm. Pump nominal speed is 1490 rpm and nominal flow is 28 l/s. Impeller installed in the pump has four vanes.

Before actual measurements were started a search for the optimal sensor location was conducted. The accelerometer measures acceleration in one direction that is perpendicular to its main surface (Figure 5-2). As was shown in Chapter 3, the major vibration components in rotating machines are radial. For that reason, the sensor should be placed on radial plane of the machine.

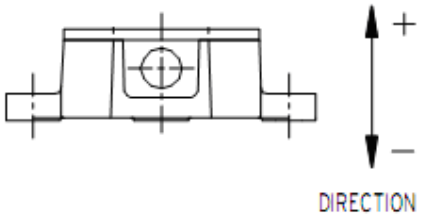

Figure 5-2 Measurement axis of accelerometer.

Several places were evaluated. One of the selection factors was the ability to clamp the sensor easily. The selected optimal position was on the motor housing (Figure 5-3). Vibration frequency spectrum measured at 1450 rpm in the chosen location is presented in Figure 5-4.

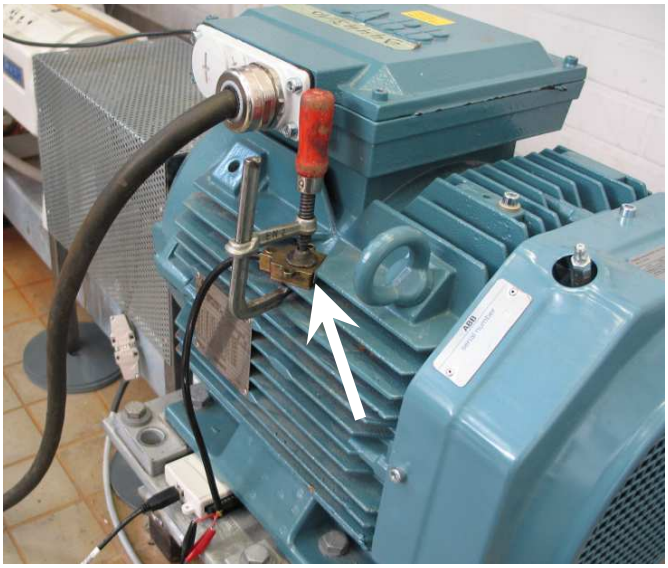

Figure 5-3 Optimal sensor location (pointed by the arrow). A clamp was applied to install the sensor on the motor's housing.

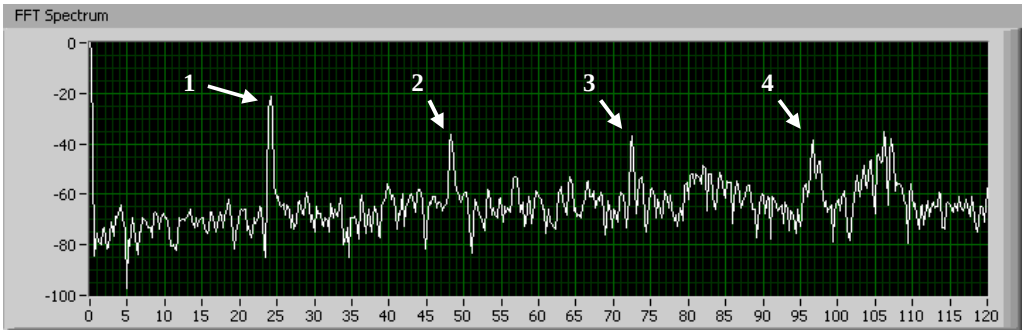

Figure 5-4 Vibration frequency spectrum measured at optimal sensor location. Measured at 1450 rpm. The major frequency component (1) stands for the rotational frequency (24Hz). Its harmonics (2,3) are also visible at 48 Hz and at 72 Hz. The vane passing frequency (4) is clearly visible at 96 Hz.

Test measurements were conducted at rotational speeds from 1100 to 1500 rpm. During the measurements the flow rate was approximately 80% of pump's best efficiency flow. For this reason the pump should operate normally. Table 5-1 presents measurement results and errors for the used algorithms. The evaluation of these measurements shows that Goertzel algorithm provides better results in most cases. The overall error for Goertzel algorithm is much smaller than for FFT. In general it should

be mentioned that both algorithms provide quite accurate results – estimated error being less than 1%.

Table 5-1 Measured rotational speed and errors for different algorithms.

Reference rotational speed, rpm	Rotational speed estimated with FFT algorithm, rpm	Rotational speed estimated with Goertzel algorithm, rpm	Relative error of FFT method	Relative error of Goertzel method	Measured flow rate, l/s
1100	1099,70	1093,20	0,03%	0,62%	15,57
1150	1139,70	1149,30	0,90%	0,06%	16,65
1200	1194,40	1195,90	0,47%	0,34%	17,40
1250	1249,00	1250,20	0,08%	0,02%	18,25
1300	1303,70	1301,10	0,28%	0,08%	19,20
1400	1413,00	1399,00	0,93%	0,07%	20,93
1450	1453,00	1449,60	0,21%	0,03%	21,77
1500	1493,00	1498,80	0,47%	0,08%	22,45
Average error =			0,42%	0,16%	

During the measurements, the motor was vibrating so strongly that after the measurements sequence, the pump and the motor were realigned. As misalignment is one of the sources for extra vibration – it may have produced additional vibration components at the frequencies 1*rpm and 2*rpm.. After the realignment the pump drive was retested at several rotational speeds. Realignment didn’t cause any significant changes in rotational speed estimation. Figure 5-5 presents vibration spectrum of the pump drive before the realignment and after it. In the later case the second harmonic of rotational frequency was significantly reduced.

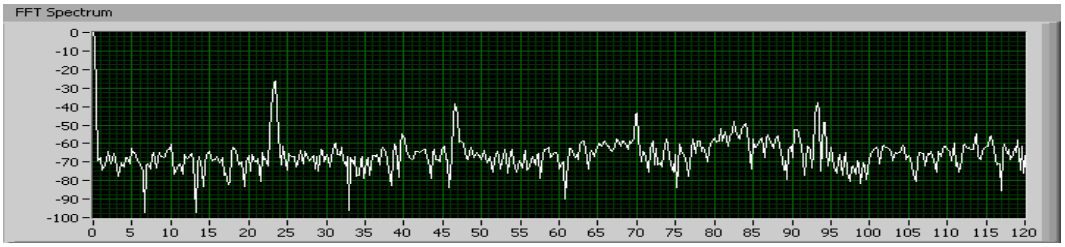

a) Before realignment

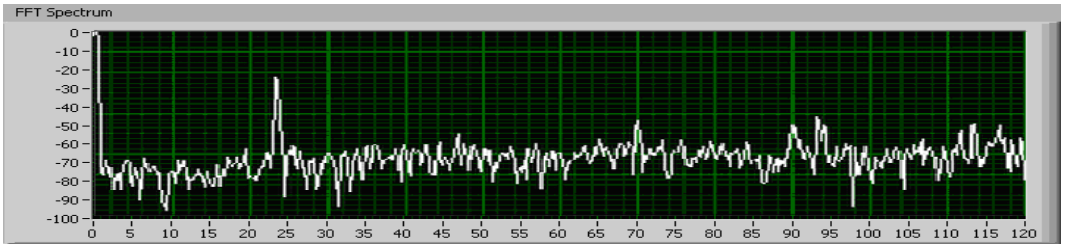

b) After alignment

Figure 5-5 Vibration spectrum of the drive measured at 1400 rpm. Realignment has significantly decreased the second harmonic of the rotational frequency at 46.6Hz. The amplitude of the main frequency was slightly increased.

5.3. Test measurement with Serlachius pump drive

Next pump drive that was tested is a combination of Serlachius DC80/260 centrifugal pump and Stromberg induction motor (Figure 5-6). The pump's impeller has five vanes. Rotational speed of the motor was adjusted by ABB ACS M1 frequency converter.

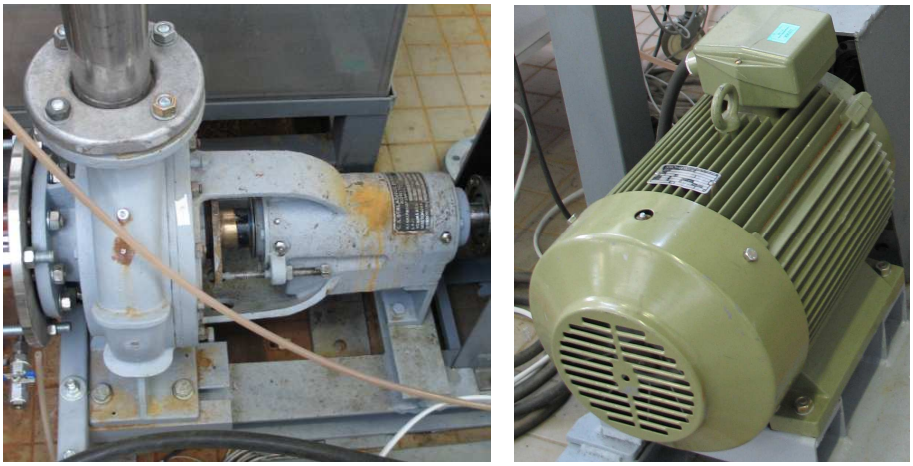

Figure 5-6 Serlachius pump drive.

Before actual measurement several positions of the sensor were evaluated. The Stromberg motor's housing doesn't provide any space to clamp acceleration sensor. The only available space on the motor is fan cover (Figure 5-7). But vibration measured in this position didn't contain significant rotational frequency component (Figure 5-8).

Figure 5-7 Accelerometer mounted on the motor cover.

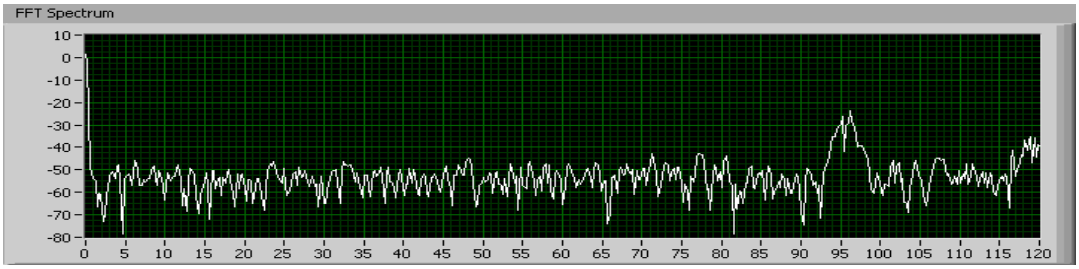

Figure 5-8 Vibration spectrum measured at the motor cover at 1425 rpm. Rotational frequency component (23.75Hz) can be hardly detected in the spectrum.

The next tested location was at the pump bearings (Figure 5-9). Measured vibration spectrum provided obvious rotational frequency component (Figure 5-10). Series of measurements at different rotation speed were conducted with this sensor position. Obtained results are presented in Table 5-2. During the measurements, the pump operated at its best efficiency flow point.

Figure 5-9 Sensor located at pump bearings. The clamp was used to mount the sensor.

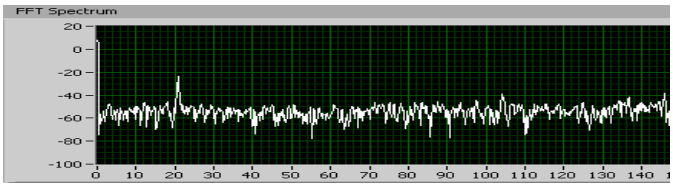

Figure 5-10 Vibration spectrum measured at pump bearings at 1250 rpm. Rotational frequency (20.8Hz) and vane passing frequency (104.1 Hz) components are visible in the spectrum.

Table 5-2 Measured rotational speed and errors for different algorithms.

Reference rotational speed, rpm	Rotational speed estimated with FFT algorithm, rpm	Rotational speed estimated with Goertzel algorithm, rpm	Relative error of FFT method	Relative error of Goertzel method	Measured flow rate, l/s
1500	1493	1500,3	0,47%	0,02%	24
1450	1453	1453,7	0,21%	0,26%	22,9
1425	1418,3	1418,2	0,47%	0,48%	23
1400	1413	1399,1	0,93%	0,06%	22,7
1350	1343,7	1351,6	0,47%	0,12%	21,6
1300	1303,7	1297,2	0,28%	0,22%	20,8
1250	1249	1250,2	0,08%	0,02%	19,9
1200	1194,4	1195,7	0,47%	0,36%	19,2
1150	1154,4	1237,2	0,38%	7,58%	18,2
1100	1099,7	1103,9	0,03%	0,35%	17,3
Average error =			0,38%	0,95%	

Presented test results show that both algorithms provide accuracy of 1%. The only case where Goertzel algorithm has an error about 8% was measured at 1150 rpm. The frequency spectrum of the measured vibration at this rotational speed is presented in Figure 5-11. In the presented spectrum it can be clearly seen that rotational component (19.1Hz) is not very distinctive. The probable reason for that is some mechanical resonance. The vane passing frequency can be clearly seen at 95.8 Hz.

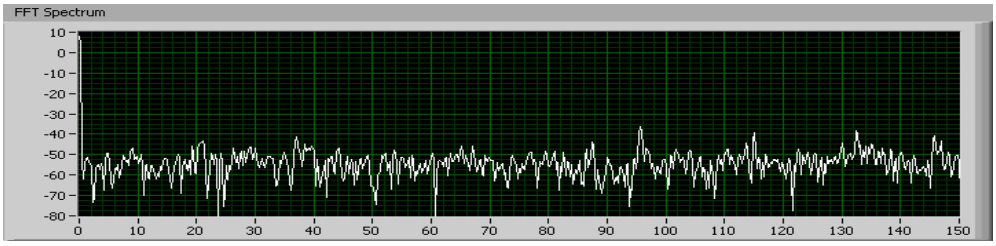

Figure 5-11 Vibration spectrum measured at 1150 rpm.

To further test the effect of sensor location several measurements were taken with a changed sensor position. Accelerometer was placed on the pump volute chamber casing (Figure 5-12).

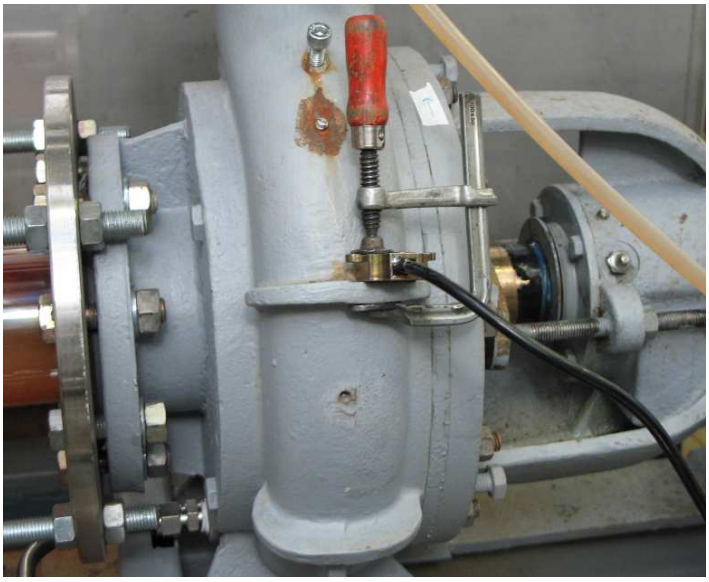

Figure 5-12 Sensor positioned on volute chamber casing. The clamp was used for mounting.

Vibration spectrum presented in Figure 5-13 was measured at 1150 rpm at the new sensor location. As in the previous case, vibration component at 20.83 Hz led to significant errors in speed estimation. The probable reason of this vibration component is some mechanical interference of the pump-motor-pipes system. The correctness of the estimated speed could be proven by VPF which is equal to 95.8 Hz thus for the five vane impeller the rotational frequency should be 19.17 Hz that is equal to 1150 rpm.

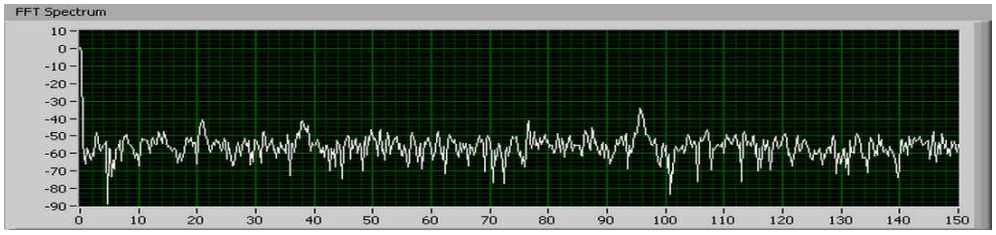

Figure 5-13 Vibration spectrum measured at volute chamber at 1150 rpm.

5.4. Test measurement with FläktWoods fan drive

The last measured machine was an axial fan drive. The measurement process was conducted in a fan laboratory in Lappeenranta University of Technology. The fan drive model is AXIPAL BZI VA630 4P manufactured by FläktWoods (Figure 5-14).

The purpose of this measurement was to test, if the developed measurement system can be applied to estimate rotational speed of fan drives. The fan drive consists of an ABB M3AA 132 BC-2 3 phase induction motor with nominal speed of 2880 rpm and a propeller that has four blades. Construction of the fan is shown in Figure 5-15.

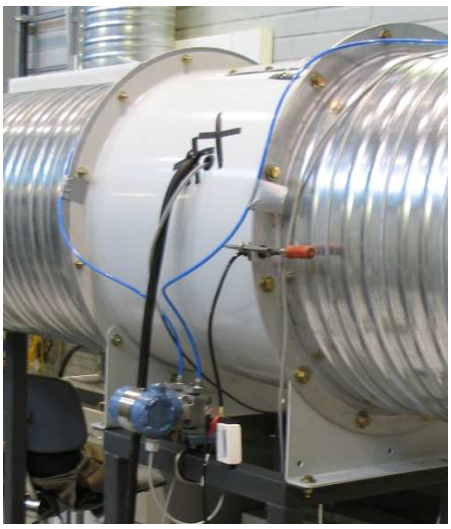

Figure 5-14 FläktWoods AXIPAL BZI VA630 4P fan drive.

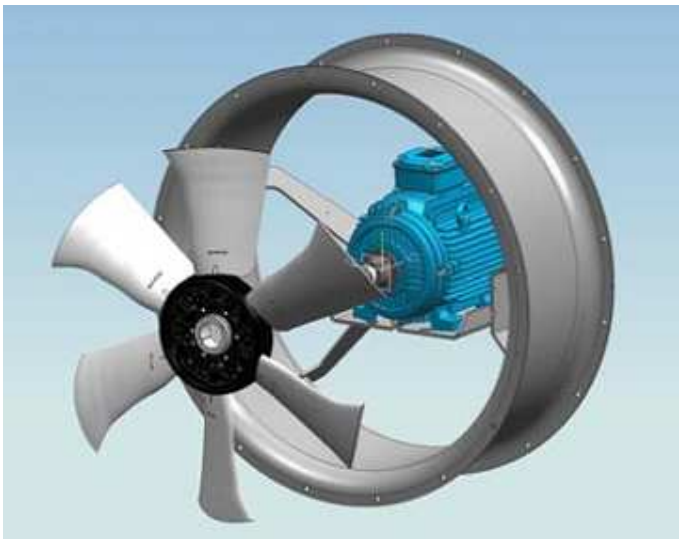

Figure 5-15 Parts of fan drive.

Several places of sensor location were evaluated. The location on fan's motor was not tested because it demanded disassembling of the fan's casing and that

contradicts with the project's idea. The first test round was conducted with the accelerometer placed on the fan drive chassis (Figure 5-16). The measurement axis of the sensor was located in parallel to the fan shaft.

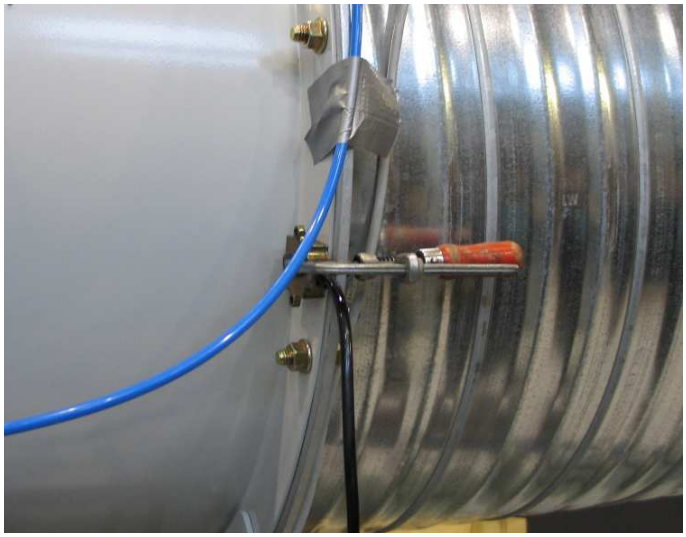

Figure 5-16 Sensor mounting in axial plane.

The measurements were conducted at rotational speeds from 1500 to 3000 rpm. Table 5-3 presents results of speed estimation.

Table 5-3 Results of speed estimation of fan drive.

Reference rotational speed, rpm	Rotational speed estimated with FFT algorithm, rpm	Rotational speed estimated with Goertzel algorithm, rpm	Relative error of FFT method	Relative error of Goertzel method	Measured flow rate, l/s
1500	1500	1504,3	0,00%	0,29%	39,6
1500	1695	1220,2	13,00%	18,65%	39,5
2400	2205	2209,4	8,13%	7,94%	65
2400	2400	2398,6	0,00%	0,06%	65
3000	3000	3002,4	0,00%	0,08%	80
3000	3015	3013	0,50%	0,43%	80

Results provided by both algorithms have a low number of errors. The reason of incorrect results is high damping ratio of the tubes connected to the fan's housing.

Another series of measurements were conducted with the sensor positioned in the radial plane as shown in Figure 5-17. In this series of measurements the value of the rotational speed was held constant. Also the fan flow rate was held constant.

Figure 5-17 Sensor mounted on fan drive chassis.

In this location of the sensor results of speed estimation had a lot of variations. The probable reason is the poor sensor position. High part of vibration components is damped by fan chassis, which has also reduced amplitude of characteristic frequencies compared with other components. The results are presented in Table 5-4. Frequency spectrum of measured signal is presented in Figure 5-18.

Table 5-4 Speed estimation results

Reference rotational speed, rpm	Rotational speed estimated with FFT algorithm, rpm	Rotational speed estimated with Goertzel algorithm, rpm	Relative error of FFT method	Relative error of Goertzel method	Measured flow rate, l/s
2400	2490	2482,1	3,75%	3,42%	65
2400	2685	2390,9	11,88%	0,38%	65
2400	2400	2393,8	0,00%	0,26%	65
2400	2400	2211,4	0,00%	7,86%	65

2400	2400	2391,8	0,00%	0,34%	65
2400	2400	2135,5	0,00%	11,02%	65
2400	2685	2405,3	11,88%	0,22%	65
2400	2460	2540,6	2,50%	5,86%	65
2400	2655	2647,2	10,63%	10,30%	65
2400	2145	2405,3	10,63%	0,22%	65
2400	2610	2420,6	8,75%	0,86%	65
2400	2355	2166,2	1,88%	9,74%	65
2400	2460	2391,8	2,50%	0,34%	65
2400	2595	2509,9	8,13%	4,58%	65
2400	2565	2286,2	6,88%	4,74%	65
2400	2160	2164,3	10,00%	9,82%	65
Average error =			5,59%	4,37%	

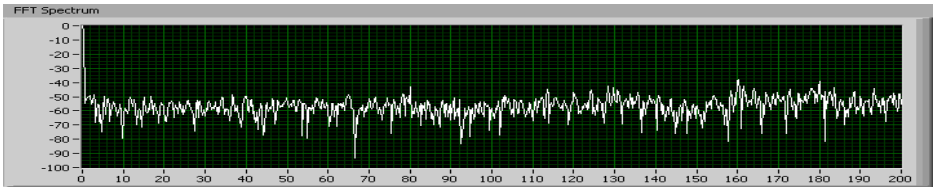

Figure 5-18 Vibration spectrum of the measured signal. Rotational component is expected at 40 Hz but not visibe. However second and fourth harmonics can be detected. The fourth harmonic is also amplified by the vane passing frequency.

5.5. Summary of the test measurements

The conducted measurements showed that although in most cases the system provides correct results, the estimation may fail sometimes. The main reason of the errors in the estimation is a non-distinctive main component in the frequency spectrum. Also the incorrect sensor installation can lead to estimation errors. But in the majority of conducted measurements, provided results were correct. Both estimation algorithms provided high level of accuracy.

The software part of the system operated correctly. The usage of database simplified the process of saving the estimation results. Predefined motor and pump databases allowed to decrease the measurement preparation time, because they provided easy way for filling in motors and pumps data. The efficiency estimation algorithm also provided correct results for measured pump drives.

6. SUMMARY AND CONCLUSION

Modern industry employs a high number of pump drive systems. These systems account for nearly 20% of the worlds electrical energy demand. They provide domestic services, commercial and agricultural services, municipal waste/water services. Also they are widely used in industrial services for food processing, chemical, petrochemical, pharmaceutical and mechanical industries. In recent decade much attention is paid to efficiency of pumping systems. As the number of employed pump drives is high, the rise in pump efficiency can lead to a high reduction in energy consumption and consequently the reduction of energy consumption. This will also lead to the decline of emissions created due to energy production. In addition to the environmental reasons, economical profit is also accounted. These factors have led to development of energy auditing techniques. These techniques are used to measure energy consumption and provide solutions for optimization.

The aim of this thesis was to develop a tool that can be used in energy auditing process. This tool should provide an easy way for measuring pump drive to determine pump drive working point location thus estimating pump's operating efficiency. The requirements for the measurement system were derived from real industry needs. The main requirements for the system were mobility, ease of use and possibility of post analysis.

During the development several measurement techniques were evaluated. For rotational speed estimation two algorithms were used in the project. Both of them provided correct results with reasonable processing power requirements. The further development of the measurement algorithm can provide more stable data results. The proposal for the development is to increase the number of characteristic frequencies that are analyzed in the speed estimation process. The analysis of test results showed that in some cases the rotational component in the vibration spectrum can not be easily located, but at the same time the vane passing frequency component is very distinctive. The algorithm should also deduct and analyze the VPF and other harmonics of the main frequency. This will let the algorithm to withstand different noise frequencies with high amplitude.

The evaluation of the measurement system operation was conducted during laboratory testing. The system was considered to be user friendly.

Current system hardware platform can be used for a future development of vibration analysis system.

As an outcome next facts can be stated with a high degree of confidence:

- The developed system provides correct measurement results
- The developed estimation techniques provide correct results
- The system can be employed in industrial measurement processes.

REFERENCES

[1] Europump, Hydraulic Institute. 2001. Pump life cycle costs: A guide to LCC analysis for pumping systems. Executive summary. [e-document]. [Retrieved 20.4.2010], From http://www1.eere.energy.gov/industry/bestpractices/pdfs/pumplcc_1001.pdf

[2] Pump Systems Matter.2009. Pumping System Optimization: Opportunities to Improve Life Cycle Performance. [e-document]. [Retrived 20.4.2010]. From: http://www.pumpsystemsmatter.org/default.aspx

[3] Ahonen T., Tamminen J., Ahola J. and Kestila J. Sensorless pump operation estimation. [e-document]. [Retrieved 20.4.2010] From: http://ieeexplore.ieee.org%2Fiel5%2F5254890%2F5278662%2F05278945.pdf

[4] Sulzer Pumps. 2009. Sulzer IntO™. [e-document] [Retrieved 20.04.2010] From: http://www.sulzerpumps.com/portaldata/9/Resources//brochures/css/IntOIntelligentObserver_E00627_fi.pdf

[5] Sahu G. K. 2007. Pumps: Theory, Design And Applications. New Age International. 320 pages

[6] Justin Bjork and Barry Erickson. 2006. Presentation “Centrifugal pumps”. [e-document]. [Retrieved 20.4.2010]. From http://www.vibration.org/Presentation/May%202006/Centrifugal%20Pumps%20May%204,%202006.pdf

[7] Fantagu. Parts of a centrifugal pump. [e-document]. [Retrieved 20.4.2010]. From http://upload.wikimedia.org/wikipedia/commons/thumb/4/4a/Centrifugal_Pump.png/585px-Centrifugal_Pump.png

[8] Sulzer. 2006. AHLSTAR A_P22-80. [e-document]. [Retrieved 20.4.2010]. From: file://d:\lut\pump\references\k13837.pdf

[9] ABB. 2010. LV Industrial performance motors catalog. [e-document]. [Retrieved 20.4.2010]. From: http://www05.abb.com/global/scot/scot259.nsf/veritydisplay/16d2d4acad96001cc12576eb004781e3/$File/IPM_9AKK104559%20EN%20Feb2010_low.pdf

[10] Paresh Girdhar and Cornelius Scheffer. 2004. Practical machinery vibration analysis and predictive maintenance. Elsevier. 255 pages. ISBN 978-0750662758

[11] Glenn Bate. Vibration diagnostics for industrial electric motor drives: Application Notes. Bruel&Kier. [e-document]. [Retrieved 20.4.2010] From: www.bksv.com/doc/bo0269.pdf

[12] I. Boldea, S. A. Nasar. 2002. The induction machine handbook. CRC Press. 950 pages. ISBN0849300045.

[13] Wikipedia. 2010. Discrete Fourier transform. [e-document]. [Retrieved 20.4.2010] From: http://en.wikipedia.org/wiki/Discrete_Fourier_transform

[14] Wikipedia. Goertzel algorithm. [e-document]. [Retrieved 20.4.2010]. From: http://en.wikipedia.org/wiki/Goertzel_algorithm

[15] Banks Kevin. 2002. The Goertzel Algorithm. [e-document]. [Retrieved 20.4.2010]. From: http://www.embedded.com/story/OEG20020819S0057

[16] LabSQL, [e-document]. [Retrieved 20.4.2010]. From: http://jeffreytravis.com/lost/labsql.html

[17] Victor Wowk, 1991. Machinery vibration: measurement and analysis Mechanical Engineering. McGraw-Hill Professional. 358 pages. ISBN 978-0070719361

[18] Yedidiah S. 1996. Centrifugal pump user's guidebook: problems and solutions. Springer. 387 pages. ISBN 9780412991110

[19] European Commission. 2001. Study on improving the energy efficiency of pumps. [e-document]. [Retrieved 20.4.2010]. From http://re.jrc.ec.europa.eu/energyefficiency/motorchallenge/pdf/SAVE_PUMPS_Final_Report_June_2003.pdf

[20] Hooker M. and Eckert T. 2005. Centrifugal Pump Vibration. [e-document]. [Retrieved 20.4.2010]. From: http://www.scribd.com/doc/19305739/Engineering-Training-Module-14-Centrifugal-Pump-Vibration

APPENDICES

Acer Aspire 2010 laptop features

Performance
Intel® Pentium® M Processor at 1.4 GHz or higher
2 memory slots supporting 333 MHz DDR, upgradeable to 2GB
30GB and up Enhanced-IDE hard disk drive
Multimedia
Built-in optical drive (DVD/CD-RW Combo or DVD-Dual Drive)
15.4” TFT Color LCD,1280x800 (WXGA) panel
2.1 channel speaker
Audio input and output jacks
Connectivity
Integrated 10/100Mbps Ethernet connection
Built-in 56Kbps fax/data modem
Three universal serial bus (USB 2.0) ports
One IEEE 1394 port
802.11b and 802.11b/g Wireless LAN and Bluetooth
Human-centric design
Rugged, portable construction
Stylish appearance
Standard 85 keys keyboard with four programmable launch key
Comfortable palm rest area with well-positioned touchpad
Expansion
PC card slot enables a range of add-on options
Upgradeable hard disk and memory modules
Display
The 15.4” display panel
ATI Radeon 9700 with 64MB DDR VGA Memory
Supports simultaneous display on external LCD or CRT
S-video for output to a television or display device that supports

NI USB-6009 DAQ Card features

General Product Name	USB-6009
Product Family	Multifunction Data Acquisition
Form Factor	USB
Operating System/Target	Windows , Linux , Mac OS , Pocket PC
DAQ Product Family	B Series
Measurement Type	Voltage
Analog Input	
Channels	8 , 4
Single-Ended Channels	8
Differential Channels	4
Resolution	14 bits
Sample Rate	48 kS/s
Throughput	48 kS/s
Max Voltage	10 V
Maximum Voltage Range	-10 V , 10 V
Maximum Voltage Range Accuracy	138 mV
Minimum Voltage Range	-1 V , 1 V
Minimum Voltage Range Accuracy	37.5 mV
Number of Ranges	8
Simultaneous Sampling	No
On-Board Memory	512 B
Analog Output	
Channels	2
Resolution	12 bits
Max Voltage	5 V
Maximum Voltage Range	0 V , 5 V
Maximum Voltage Range Accuracy	7 mV
Minimum Voltage Range	0 V , 5 V
Minimum Voltage Range Accuracy	7 mV
Update Rate	150 S/s
Current Drive Single	5 mA
Current Drive All	10 mA
Physical Specifications	
Length	8.51 cm
Width	8.18 cm
Height	2.31 cm
I/O Connector	Screw terminals

SCA111-C12H1W features

SCA111-C12H1W electrical characteristics

Parameter	Comment	Value	Units
Sensitivity error	At room temperature	±2	%
	-20…85°C	±3	
	-40…125°C	±4	
Typ. Non-linearity	Deviation from ±1g line	±20	mg
Frequency response	-3dB point	400± 150	Hz
Output load	resistive (min)	20	kl
	capacitive (max)	20	nF
Supply voltage effect	offset	±25	mg
Cross-axis sensitivity		±4	%
Typ. output noise	V(AC) RMS (DC…4kHz)	5	mV
Radiometric error	Vdd=4.75..5.25V	±2	%

SCA111-C12H1W performance characteristics

Parameter	Comment	Value	Unit
Supply voltage	Radiometric	7-27	V
Supply current	Typical without load	2	mA
Measuring range		±1.2	g
Measuring direction		Horizontal	
Zero point	Nominal value	2.5	V
Sensitivity	Nominal value	1.5	mg

Dimensions of SCA111-C12H1W